Food Hydrocolloids 142 (2023) 108813

Contents lists available at ScienceDirect

Food Hydrocolloids

journal homepage: www.elsevier.com/locate/foodhyd

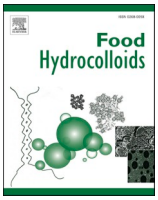

Development of biodegradable and vermicompostable films based on alginate and waste eggshells

Valeria Villanueva [a], Fabrizzio Valdés [a], Rommy N. Zúñiga [b], María Gabriela Villamizar-Sarmiento [c], Eduardo Soto-Bustamante [d], Patricio Romero-Hasler [d], Ana Luisa Riveros [e], Jose Tapia [f], Judit Lisoni [f], Felipe Oyarzun-Ampuero [c], Carolina Valenzuela [a,*]

[a] Departamento de Fomento de la Producción Animal, Facultad de Ciencias Veterinarias y Pecuarias, Universidad de Chile, Santa Rosa 11.735, La Pintana, Santiago, Chile
[b] Laboratorio de Ingeniería en Bioprocesos, Departamento de Biotecnología, Universidad Tecnológica Metropolitana, Las Palmeras 3360, Ñuñoa, Santiago, Chile
[c] Departamento de Ciencias y Tecnología Farmacéuticas, Facultad de Ciencias Químicas y Farmacéuticas, Universidad de Chile, Santos Dumont 964, Independencia, Santiago, Chile
[d] Departamento de Química Orgánica y Fisicoquímica, Facultad de Ciencias Químicas y Farmacéuticas, Universidad de Chile, Olivos 1007, Independencia, Santiago, Chile
[e] Departamento de Química Farmacológica y Toxicológica, Facultad de Ciencias Químicas y Farmacéuticas, Universidad de Chile, Santos Dumont 964, Independencia, Santiago, Chile
[f] Instituto de Ciencias Físicas y Matemáticas, Facultad de Ciencias, Universidad Austral de Chile, Valdivia, Región de Los Ríos, Chile

ARTICLE INFO

Keywords:
Alginate
Biodegradable
Eggshell
Films
Vermicomposting
Waste eggs

ABSTRACT

The development of biofilms to replace plastics is urgent, due to the high environmental pollution caused by the non-biodegradable packaging. The objective of this study was to develop and understand the behavior and properties of biodegradable films based on an alginate/glycerol matrix with eggshell waste. Eggshells were transformed to eggshell powder (EP) and this ingredient used to obtain EP biodegradable films (EPBFs) using the casting method. EP contributed opacity and whitish coloration to the EPBFs. Stress-strain curves show that EP content significantly influences mechanical properties; resulting in harder, firmer and less elastic EPBFs with increasing EP content. The EPBFs had heterogeneous and rough surfaces with crystalline forms provided by EP with a particle size distribution ranged from 20.7 to 26.6 μm, arranged as a monolithic pattern with very low porosity. EPBFs were amorphous materials and WAXS analysis indicated that $CaCO_3$ content ranged 18–50% in the EPBFs. Thermal decomposition processes of the EPBFs, was not affected by the EP addition at concentrations below 6%. The addition of EP increased the hydrophobicity of EPBFs, slowing solubilization in water; however, the water solubility percentage was high (82.9% for EPBF-2%–75.2% for EPBF-6%). EPBFs completely biodegrade in vermicomposting in short periods of time (between 14 and 21 days). In conclusion, EPBFs, derived from waste, constitute an interesting new material with desirable mechanical properties for potential use as food coatings or packaging. The biodegradable properties of EPBFs allow easy disposal by dissolving in water or by vermicomposting.

1. Introduction

Several million tons of olefin-derived plastics are produced annually worldwide, accumulating in the ecosystem at a staggering rate of 300–400 million tons per year. Non-biodegradable plastic packaging is the greatest source of waste globally (Chamas et al., 2020; UNEP United Nations Environment Programme, 2022). Plastics persist for hundreds to thousands of years polluting land, water and air (Barnes, 2002; Jambeck

* Corresponding author. Casilla 2, Correo 15, La Granja, Santiago, Chile.
E-mail addresses: valeria.villanueva@veterinaria.uchile.cl (V. Villanueva), fabrizziovaldesr@gmail.com (F. Valdés), rzuniga@utem.cl (R.N. Zúñiga), magabrielavillamizarsarmiento@gmail.com (M.G. Villamizar-Sarmiento), esoto@ciq.uchile.cl (E. Soto-Bustamante), patricio_romero@outlook.com (P. Romero-Hasler), ana.riveros@ciq.uchile.cl (A.L. Riveros), cote923@gmail.com (J. Tapia), judit.lisoni@uach.cl (J. Lisoni), foyarzuna@ciq.uchile.cl (F. Oyarzun-Ampuero), cvalenzuelav@u.uchile.cl (C. Valenzuela).

https://doi.org/10.1016/j.foodhyd.2023.108813
Received 2 January 2023; Received in revised form 12 April 2023; Accepted 24 April 2023
Available online 2 May 2023

et al., 2015; Lavers, Stivaktakis, Hutton, & Bond, 2019). Plastic pollution is the reason for growing global concern and programs that promote the use of strategies that manage plastic waste, including disposal, recycling and incineration, which also affect environmental pollution associated with greenhouse gas emissions (Al-Salem, Lettieri, & Baeyens, 2009; Elsabee & Abdou, 2013; Moharir & Kumar, 2019; Verma, Vinoda, Papireddy, & Gowda, 2016; Wright & Kelly, 2017).

In recent years, the development of biodegradable packaging to replace plastics has become a hot topic (Chia, Ying Tang, Khoo, Kay Lup, & Chew, 2020; Flury & Narayan, 2021; Stoica, Marian Antohi, Laura Zlati, & Stoica, 2020). The potential benefits of biodegradable films are that they are edible, water-soluble, non-toxic, renewable, biocompatible and compostable (Bonilla & Sobral, 2020; Dehghani, Hosseini, & Regenstein, 2018; Oluic & Holmquist, 2021) and vermicompostable (Samal, Raj Mohan, Chaudhary, & Moulick, 2019). The vermicomposting properties of biodegradable films is the least studied, and is based on the rapid degradation of organic matter by the action of a symbiotic system between earthworms and microorganisms (Alshehrei & Ameen, 2021). Vermicomposting is a highly sustainable system for organic waste disposal in a short time, which is low cost, and eco-friendly (Bhat et al., 2018; Hazarika & Khwairakpam, 2022; Sharma & Garg, 2017), due to less methane emission than composting (Sharma & Garg, 2019; Swati & Hait, 2018). Vermicomposting does not produce waste and/or residues. Remarkably, vermicompost is a nutrient-rich organic material that is commonly used as a natural fertilizer (Ghorbani & Sabour, 2021; Raza, Wu, Rene, Ali, & Chen, 2022; Zhou, Li, Guo, Liu, & Cai, 2022).

Biodegradable films have been prepared using mixtures of carbohydrates, proteins, lipids, waxes, and plasticizers (Abera, Woldeyes, Demash, & Miyake, 2020; Molavi, Behfar, Ali Shariati, Kaviani, & Atarod, 2015; Vattanagijyingyong, Yonemochi, & Chatchawalsaisin, 2021; Vinod, Sanjay, Suchart, & Jyotishkumar, 2020; Wang, Ding, Ma, & Zhang, 2021). Specifically, for food and medical packing, biodegradable film composition must include chemical, biological and physical protection (El Bourakadi, Mekhzoum, Qaiss, & Bouhfid, 2021). Although carbohydrates have good filmogenic properties, films made from carbohydrates are usually stiff and brittle with low adhesiveness (Roy & Rhim, 2020; Shankar, Wang, & Rhim, 2017). Therefore, it is necessary to combine carbohydrates with other components, such as proteins and/or plasticizers (which alone do not have film-forming properties), to obtain materials with the desirable mechanical properties (i.e. flexibility, strength, elongation, hardness), able to adhere to surfaces and/or contours, and to be used as coatings (Dong, Chen, Qiao, & Liu, 2019; Pavlath & Orts, 2009). When lipids are added to biopolymer blends, usually to improve the permeability of water vapour or gases, the resistance of biodegradable films tends to be reduced (Valenzuela, Abugoch, & Tapia, 2013).

Sodium alginate is an outstanding candidate as a biopolymer in film design. Alginate is a colloidal anionic polysaccharide extracted from brown algae with biocompatibility, stability, and gelation and film-forming ability (Luo, Liu, Yang, Zeng, & Wu, 2019; Marangoni Júnior, Rodrigues, da Silva, Vieira, & Alves, 2021). However, when alginate is used alone, films show low resistance to fracture and elongation (Abdollahi, Alboofetileh, Rezaei, & Behrooz, 2013; Chen et al., 2021; Naidu & John, 2021; Yang, Shi, & Xia, 2018).

Our research group is interested in the use of hen eggshells as a low-cost material that could improve the mechanical properties of biodegradable films. Eggshells have a bio-ceramic composition with high mechanical strength (3 kgf/cm^2) (Taylor, Walsh, Cullen, & O'Reilly, 2016), due to the high concentration of calcium carbonate (96%) (Gautron et al., 2021; Gbadeyan, Adali, Bright, Sithole, & Awogbemi, 2020). Interestingly, a variety of studies have used calcium carbonate, from origins other than eggshells, with the aim of improving the strength of films (Lin, Chen, Chan, & Wu, 2008; Liu, Tian, Jia, & Zhang, 2008). Globally, large volumes of eggshell waste are generated in food processing industries and in households (Sathiparan, 2021; Waheed et al., 2020). For example, in the US, more than 45 million kg/year of eggshells are disposed of as waste (Yoo, Hsieh, Zou, & Kokoszka, 2009). Interestingly, discarded eggshells also contain albumin (Guo, Xu, Xu, Cheng, & Ding, 2021; Jalili-Firoozinezhad, Filippi, Mohabatpour, Letourneur, & Scherberich, 2020) and membrane proteins, which could confer greater elasticity to films (Han, Liu, Liu, Huang, & Sheng, 2020; Mohammadi et al., 2018). Some authors have used eggshells as a bio-filler for coating materials (Seeharaj, Sripako, Promta, Detsri, & Vittayakorn, 2019; Wen, Huang, & Guo, 2019; Yew, Ramli Sulong, Yew, Amalina, & Johan, 2013), to create nanocomposites (Rahman, Netravali, Tiimob, & Rangari, 2014), and thermoplastic materials (Bootklad & Kaewtatip, 2013). These materials show significant improvements in Young's modulus, tensile strength, and thermal stability over calcium carbonate; providing enhanced resistance to mechanical stress. In an interesting study by Vonnie et al. (2022), mixtures of eggshell powder (EP) and corn-starch were used to develop a film with a smooth structure, no cracks, and evidence of a large surface area. The authors believe the chemical composition of the O–C–O bond in the calcium carbonate of the eggshell is the main reason for the improvement in physical properties such as moisture content, swelling power, water solubility, and water absorption.

The motivation for this study was to develop films with desirable physical, mechanical and biodegradable characteristics following a low-cost and simple process, with raw hen eggshell as the key waste ingredient. The objective of this study was to develop and understand the behavior and properties of biodegradable films based on an alginate/glycerol matrix with eggshell waste.

2. Material and methods

2.1. Materials

Sodium alginate (viscosity 30 cps at 25 °C, CAS 9005-38-3, Cat. no W201502, molecular weight 12–40 kDa, Sigma-Aldrich, USA) and glycerol (≥95% purity, COPROLAN, Chile) were used to prepare the biodegradable films. Raw white hen eggshells containing remains of albumin and shell membranes were used. Eggshells were collected from household wastes. Eggs were obtained from supermarkets and local fairs. Eggshells were frozen at −18 °C in Ziploc® plastic bags to stop microorganism activity until processing.

2.2. Preparation and characterization of eggshell powder (EP)

Eggshells were defrosted at refrigeration temperature (4–6 °C), transferred on aluminum trays and oven-dried at 70 °C for 4 h. Then the eggshells were ground 3 times for 10 s (70 rpm and room temperature) in a food processor (HuromChef®, Hurom, Chile) to produce EP. The particle size distribution of EP was determined by a laser scattering particle size distribution analyzer (Partica LA-960, HORIBA Scientific, Kyoto, Japan). Briefly, 1 g of sample was suspended in 10 mL of Milli-Q water and introduced in the measurement cuvette at 25 °C. During the measurement ($n \geq 3$), a 650 nm laser diode passed through the particle suspension under magnetic stirring; the scattered light was detected and collected by a silicon photo diode detector.

EP characterization in terms of dry matter, crude protein, ether extract, ash, crude fiber, nitrogen-free extract and calcium, was conducted according to the Association of Official Analytical Chemists (AOAC) guidelines (AOAC Association of Official Analytical Chemists, 1996). Briefly, dry matter was determined gravimetrically (method 934.01). Crude protein was analyzed by the Kjeldahl method (981.10). Ether extract was determined using Soxhlet extraction (method 991.36). Ash content was determined gravimetrically (method 920.153). Crude fiber was determined by successive hydrolysis (method 993.19); nitrogen-free extract was calculated as the difference. Calcium determinations were conducted according AOAC Association of Official Analytical Chemists (1996) standards, with an inducted coupled plasma analysis (Thermo-Fisher Scientific Corp., Pittsburgh, PA, USA).

2.3. EP biodegradable film (EPBF) preparation

The EP was suspended in a solution of 2% w/v sodium alginate in distilled water at different concentrations: 0 (control film), 2, 4 and 6% EP w/v. Then, glycerol at 5% v/v was added. The dispersions were stirred for 3 h in a paddle homogenizer (Bosch MSM6A3R 750w, China), then subjected to ultrasound (Elma, Elmasonic E30H, Germany) for 30 min, and left overnight at 4 °C to eliminate bubbles. EPBFs were prepared by the casting method as described by Valenzuela, Abugoch, and Tapia (2013) and Valenzuela, Abugoch, Tapia, et al. (2013). Briefly, 20 mL of EPBF-forming dispersions were cast on a horizontal surface in low density polyethylene boxes (10 cm diameter) and oven-dried at 40 °C, to a constant weight (approximately 16 h). The dried EPBFs were removed carefully from the boxes and placed on vinyl adhesive paper in a glass desiccator with silica gel beads. The acronyms used for the obtained biodegradable films are: EPBF-0% (control, without EP), EPBF-2% (2% w/v EP), EPBF-4% (4% w/v EP) and EPBF-6% (6% w/v EP).

2.4. Characterization of EPBFs

2.4.1. Appearance and color

The appearance of the EPBFs was captured using a Sony DSC-HX1 (Sony Corporation, Japan) digital camera. The color was measured and registered in triplicate according to the Lab color scale (N = 30 for each replicate) with a colorimeter (CR-300 Konica Minolta Inc, Japan).

2.4.2. Mechanical properties

The tensile properties of the EPBFs were obtained from the stress-strain curves characterized with a universal testing machine (Brookfield CT3-1000 Texture Analyzer, USA) with 1 kg of maximum loading, a Brookfield Texture PRO CT® software control, and a test speed of 20 mm/min. As there was an abrupt change in the mechanical properties of the samples between 0% and 2% EP, we additionally developed EPBFs with 0.5%, 1.0% and 1.5% EP. For each composition, three different EPBFs were measured. Strips of 10 mm (width) x 50 mm (length) were taken from the center part of each EPBF and measured using the TA-DGA fixture configuration where the material is double clamped at an initial separation of 40 mm, value used as initial distance for the strain determination. The cross-sectional area "A" (in mm^2) was obtained by measuring the thickness of the strips with a micrometer (10 μm resolution); the thickness values reported are the average of three points per sample. The tensile strength (TS) and percent of elongation at break (EAB%) are defined in Equations (1) and (2), respectively. The range of the apparent Young's Modulus is given at 10% elongation ($YM_{10\%}$), as defined in Equation (3). $YM_{10\%}$ is used for a semi quantitative comparison of strength between samples; the elongation condition of 10% is considered the lowest yield strength observed in the EPBF-6% sample. Toughness is computed as the area under the stress-strain curve before rupture.

$$TS\ (MPa) = \frac{F}{A} = \frac{10^6 F(N)}{10\ (m) * thickness\ (m)} \quad (1)$$

Where: F is the force maximum at rupture of the EPBF (in N) and A is the cross-sectional area in m^2

$$EAB\% = \frac{D_f - 40\ mm}{40mm} \times 100\% \quad (2)$$

Where: D_f is the distance elongation at break (mm)

$$YM_{10\%}(MPa) = \frac{Stress(at\ 10\%\ elongation)}{0.1} \quad (3)$$

2.4.3. Microstructural properties

The optical microscopy was performed in a Bresser Trino Researcher II (4–10 ×) trinocular microscope (Rhede, Germany), coupled with a 5 Mp CCD color camera (Bresser, Rhede, Germany) and with a cold light source Optika CL-41 (Ponteranica, Italy).

Top views and cross sections of the EPBFs were observed by Field Emission Scanning Electron Microscopy (FE-SEM) (GeminiSEM 360, Carl Zeiss AG, Oberkochen, Germany), with a Gemini 1 optic InLens detector, which ensures an efficient signal detection for both secondary (SE) and backscattered (BSE) electrons. Parallel to FE-SEM imaging, Energy Dispersive X-ray Spectroscopy (EDX) was completed using an Ultim Max 40 detector (OXFORD Instruments, High Wycombe, UK) to perform elemental analysis on the sample surface. These samples were coated with 8 nm of gold to improve the image resolution using an argon sputter coater (model 108 AUTO, Cressington Scientific Instruments Ltd., Watford, UK). For the energy dispersive X-ray spectroscopy measurements (EDS, Ultradry Pathfinder Alpine 129 eV, Thermo Fisher Scientific), the EPBFs were gold-sputter-coated in an argon atmosphere (Sputter Coater Cressington TEDPELLA, 108). Coated samples were examined with an EDS detector by FE-SEM (INSPECT-F50, Thermo Fisher Scientific, FEI) using an accelerating voltage of 25 kV. The size distribution was determined using ImageJ, 1.5 software in a population of 200 particles. Since the orientation of the particle is typically random, the diameter was measured at a fixed angle for all particles in each sample. The data obtained were represented as a histogram of frequency *vs.* size. The statistical analysis was completed with SigmaPlot, 12 software.

The EPBFs topography was obtained by Atomic Force Microscopy (AFM), using a CoreAFM from Nanosurf Inc. (Woburn, MA, USA) in intermittent contact mode. Additionally, the force spectroscopy was performed using a tip specially designed for this purpose (PPP-FMR from NanoWorld AG., Liestal, Switzerland). Images were treated using the offline freeware Gwyddion 2.42.

To determine porosity in EPBF samples, nitrogen adsorption/desorption isotherms were generated at − 196 °C in a relative pressure range of p/p^0 = 0–1 in a Micromeritics 3Flex apparatus. Prior to the analyses, the samples were degassed under vacuum at 120 °C for 4 h in a Micromeritics Smart VacPrep device. The N_2 isotherm data were used to determine the specific surface areas applying the BET model (Brunauer, Emmett, & Teller, 1938) with the Rouquerol criterion; the total pore volume (VT) calculated at p/p^0 = 0.99. The pore volume was determined from CO_2 adsorption at 273K using the Micromeritics 3Flex apparatus.

2.4.4. Powder X-ray diffraction (PXRD) and two-dimensional wide-angle X-ray scattering (2D WAXS)

X-ray diffraction is a technique used for determining atomic structure: consisting of constructive interference of a wave from a X-ray incident beam in relation to uniform atomic spacing. In this technique Bragg's law is applied, defined by $n\lambda = 2d\text{sen}\boldsymbol{\theta}$, where $n\lambda$ must fit the condition to be an entire value of wavelengths generated by a specific target to afford the constructive interference at a $2\boldsymbol{\theta}$ angle, allowing the determination of the interplanar distances (d) for each crystalline plane. PXRD was carried out in a two-circles Stoe Stadi-P diffractometer in transmission geometry with a PSD detector. The source was a line focus copper radiation monochromated with germanium (wavelength Cu $K\alpha_1$ = 1.5406 Å) at 40 kV and 30 mA. The sample was cut and stacked as 4 layers, confined between mylar films, and subject to rotation in the plane of the film. The diffractograms were between 0 and 70° with a step size of 0.1° and 1050 s per step and then added up. 2D WAXS was carried out in an Anton Paar SAXSPoint 2.0 SAXS/WAXS/GISAXS system, with an Eiger R 1M detector and a Primus100 microfocus copper source at 50 kV 100 μA monochromated by an ASTIX multilayer mirror (wavelength $CuK\alpha_{1\text{-}2}$ = 1.5418 Å) yielding point collimation. The sample was directly mounted as a single layer on a transmission sample holder and measured in a static vacuum. WAXS was measured at the sample detector distance of 116.8 mm, averaging 24 frames of 300 s exposure each time.

2.4.5. Fourier transform infrared spectroscopy (FTIR)

FTIR analyses were performed on EP and EPBFs. An ATR/FTIR Interspec 200-X spectrometer (Interspectrum OU, Estonia) provided FTIR spectra for each sample. Spectroscopic measurements were performed directly using the PIKE Miracle TM accessory in a Ge single reflection crystal plate. A concave tip was used for all FTIR spectra. An average of 20 scans over the spectral range of 600 to 4000 cm^{-1} yielded each spectrum.

2.4.6. Thermal characterization

The thermal behavior of the EPBFs was studied using Modulated Differential Scanning Calorimetry (MDSC) with a TA Q20 DSC using sealed aluminum pans (TA T-Zero pans), under nitrogen purge (50 mL/min), with a modulation amplitude of 1.5 °C/min each 90 s and a heating rate of 1.5 °C/min. The DSC was calibrated using indium (156.6 °C) at a rate of 10 °C/min. As control we used three different temperature standards: benzophenone (ME18870) m.p. 47.9 ± 0.2 °C; benzoic acid (ME18555) m.p. 122.3 ± 0.2 °C and caffeine (ME18872) m.p. 236.0 ± 0.3 °C.

The Thermogravimetric Analysis (TGA) of the EPBFs were done on a TG 209 F1 Iris Netzsch analyzer (Germany). A sample of approximately 15 mg was used in each determination. The samples were chopped in mm size bits to increase the surface area and were heated under nitrogen flow (20 mL/min) with a heating speed of 10 °C/min, in the temperature range of 25 °C–1000 °C. The thermal behavior was recorded in the TGA and Differential Thermogravimetry (DTG) modes.

2.4.7. Biodegradability properties

2.4.7.1. Contact angle measurements. Contact angle between ultra-pure water (resistivity 15.0 MΩ-cm) and EPBFs at 20 ± 0.1 °C were measured using a goniometer (Ramé-Hart Inc., model 250-F4, NJ, USA). The EPBFs were cut into rectangles (7 cm long and 1 cm width) and pasted with tape onto the leveling stage of the goniometer. Drops (1.0–1.5 μL) of ultra-pure water were manually deposited over the film surface using a precision microliter syringe (Ramé-Hart Inc., NJ, USA). At least 20 right and left contact angles were measured automatically by the equipment software (DROPimage Advanced, USA).

2.4.7.2. Solubility test. The EPBFs were subjected to a solubility test to measure their ability to dissolve in potable water (simulating household disposal conditions). This analysis was based on Gontard, Guilbert, and Cuq (1992), with some modifications. EPBF samples in the round disc shape (2 cm diameter) were cut and weighed (n = 4). Then, each disc was separately put in a beaker with 80 mL of potable water and subjected to magnetic stirring for 12 h at 25 °C. The discs were dried in an oven (25 °C for 24 h) and weighed. The water solubility percentage was calculated according to the following equation (Dick et al., 2015):

$$WS\% = \frac{W_i - W_f}{W_i} \times 100\% \quad (4)$$

Where: WS% is water solubility percentage, W_i is the initial dry weight and W_f is the final dry weight.

2.4.7.3. Biodegradability test in vermicomposting. Biodegradability testing was performed according Vig, Singh, Wani, and Singh Dhaliwal (2011) with some modifications. A nucleus of 370 adult earthworms (*Eisenia foetida*) was obtained from the vermiculture station of the Faculty of Veterinary and Livestock Sciences, University of Chile (Santiago, Chile). The nucleus was divided into four groups of 80 earthworms, each group weighed an average of 29 g. All earthworms used were adults, measuring no less than 7 cm in length, with the presence of clitellus. Four rectangular plastic boxes 34 × 20 × 12 cm^3 were filled with 415 g of substrate (horse manure and organic household waste such as fruits and vegetables). The boxes were covered with a jute fabric and the earthworms were kept for 7 days in this system for acclimatization, spraying them with 100 mL of water every two days. The biodegradability test in vermicomposting was done according to Bandyopadhyay, Saha, Brodnjak, and Sáha (2019) with some modifications. Four rectangular pieces of EPBFs were cut (40 mm × 50 mm) and weighed in triplicate. The EPBFs were buried in the box at a depth of 1 cm of substrate for four weeks. During this period, organic household waste (from fruits and vegetables) was also added as food for the earthworms. The buried films were removed from the substrate, cleaned to remove substrate debris and weighed every 7 days. The weight loss percentage of the films was calculated using the equation described by di Franco, Cyras, Busalmen, Ruseckaite, and Vázquez (2004):

$$WL\% = \frac{W_i - W_t}{W_i} \times 100\% \quad (5)$$

Where: WL% is weight loss, W_i is the initial weight and W_t is the final weight at a predetermined time t.

2.5. Statistical analysis

All analyses were performed in triplicate. The statistics used were mean ± standard deviation. These data showed a normal distribution (Shapiro Wilk test) and homoscedasticity (Levene's test); therefore, statistical analysis was performed by ANOVA analysis and Tukey's test ($p < 0.05$), using the Stadistix 8® program (AOAC Association of Official Analytical Chemists, 1996; USA).

3. Results and discussion

3.1. EP production and characterization

Dry EP showed the following proximate chemical composition: crude protein 5.9 ± 0.4%, crude fiber 1.6 ± 0.2% and ash 91.5 ± 0.5%. As expected, the main component of EP was ash, since eggshells consist of 96% calcium carbonate in the form of calcite, the remaining 3–4% are organic materials (Her, Park, Li, & Bae, 2022). The second component of importance was protein, which was identified in greater amounts than reported by other authors (Masuda & Hiramatsu, 2007). This is probably because shell membranes were not removed in this study (we try to mimic the common discarded raw material), whose composition is mainly protein (83% crude protein on dry basis) (Long, Adams, DeVore, & Franklin, 2004) including collagen and keratin. In addition, the eggshells contained traces of albumen, which has a protein content of 90% on dry basis (Campbell, Raikos, & Euston, 2003). The percentage of crude fiber was low; traces of uronic acids and dermatan sulfate present in eggshell and membranes could be considered fiber (Lunn & Buttriss, 2007; Nakano, Ikawa, & Ozimek, 2003). As expected, the calcium content of EP was high (36.7 ± 0.9 g/100 g) and similar to values reported by other authors (34–38 g) (Al-awwal & Ali, 2015; Masuda & Hiramatsu, 2007).

After grinding, the average particle size of EP was 41 ± 1 μm which is similar to other investigations that use trituration (manual/food processor) as a preparation method, giving a size range between 38 and 75 μm (Ferraz, Gamelas, Coroado, Monteiro, & Rocha, 2018; Shiferaw, Habte, Thenepalli, & Ahn, 2019). Particle size plays an important role in the properties of biodegradable films, since the interfacial region increases as the particle size decreases (Agrawal, Thakur, & Singh, 2021). In previous studies, an increase in particle size generated a decrease in Young's modulus, due to a decrease in the specific area of the particles, which reduces surface interactions and cross-linking of the material (Douce, Boilot, Biteau, Scodellaro, & Jimenez, 2004). Lower sizes could only be obtained using a combination of techniques such as ball milling, centrifugation and ultrasonication, which are more expensive and energy consuming (Iyer & Torkelson, 2014; Rahman et al., 2014).

Raw eggshells represent an interesting ingredient for our purposes.

In addition to the simplicity for collection (waste in several industries), it possesses components potentially advantageous to provide desired mechanical properties to films (*i.e.* proteins) (Han et al., 2020; Mohammadi et al., 2018; Pavlath & Orts, 2009). In addition, the EP production method is advantageous, particularly for industries requiring homogenous particle size through simple, low-cost techniques.

3.2. EPBFs characterization

3.2.1. Appearance and color

Four different formulations of EPBFs were developed: EPBF-0%, EPBF-2%, EPBF-4% and EPBF-6% (Fig. 1 and Video 1 supplementary data). Fig. 1A shows the appearance of the EPBFs; EPBF-0% was transparent, smooth, with a homogeneous surface, typical of alginate/glycerol films (Avella et al., 2007; Benavides, Villalobos-Carvajal, & Reyes, 2012; Jost, Kobsik, Schmid, & Noller, 2014; Kok & Wong, 2018; López et al., 2015). In contrast, EPBF-2%, EPBF-4% and EPBF-6% show progressively more heterogeneous surfaces, increasing the opacity and whitish coloration. These observations were analyzed with the color parameters (Table 1), where *Y* parameter (related to brightness) has a lower value for EPBF-0% and increases as the EP content increases. EP generates opacity due to the white-colored bioceramic characteristics of the added EP particles. The *X* and *y* parameters are similar for the EPBFs

Table 1
Properties of alginate/glycerol biodegradable films with different concentrations of eggshell powder (EP) of 0 (EPBF-0%), 2 (EPBF-2%), 4 (EPBF-4%) and 6% w/v (EPBF-6%).

Properties	EPBF-0%	EPBF-2%	EPBF-4%	EPBF-6%
Color parameters				
Y	5.8 ± 2.2^{a}	20.3 ± 5.4^{b}	34.5 ± 4.9^{c}	36.9 ± 5.6^{d}
X	0.316 ± 0.006^{a}	0.313 ± 0.003^{b}	0.320 ± 0.002^{b}	0.323 ± 0.003^{b}
y	0.330 ± 0.005^{a}	0.333 ± 0.003^{b}	0.338 ± 0.002^{b}	0.341 ± 0.003^{b}
Mechanical properties				
TS (MPa)	80.3 ± 10.1	193.3 ± 22.5	189.6 ± 18.5	217.2 ± 49.5
EAB% (%)	59 ± 3	31 ± 3	31 ± 6	27 ± 3
$YM_{10\%}$(GPa) range	0.03–0.07	0.15–0.22	0.20–0.27	0.25–0.44
Solubility properties				
Contact angle (°)	27.4 ± 2.2^{a}	27.9 ± 3.0^{a}	68.4 ± 4.8^{b}	62.3 ± 2.7^{c}
Water solubility (%)	90.7 ± 1.4^{a}	82.9 ± 4.4^{b}	80.3 ± 3.9^{b}	75.2 ± 8.6^{b}

Different letters indicate significant differences ($P < 0.05$).

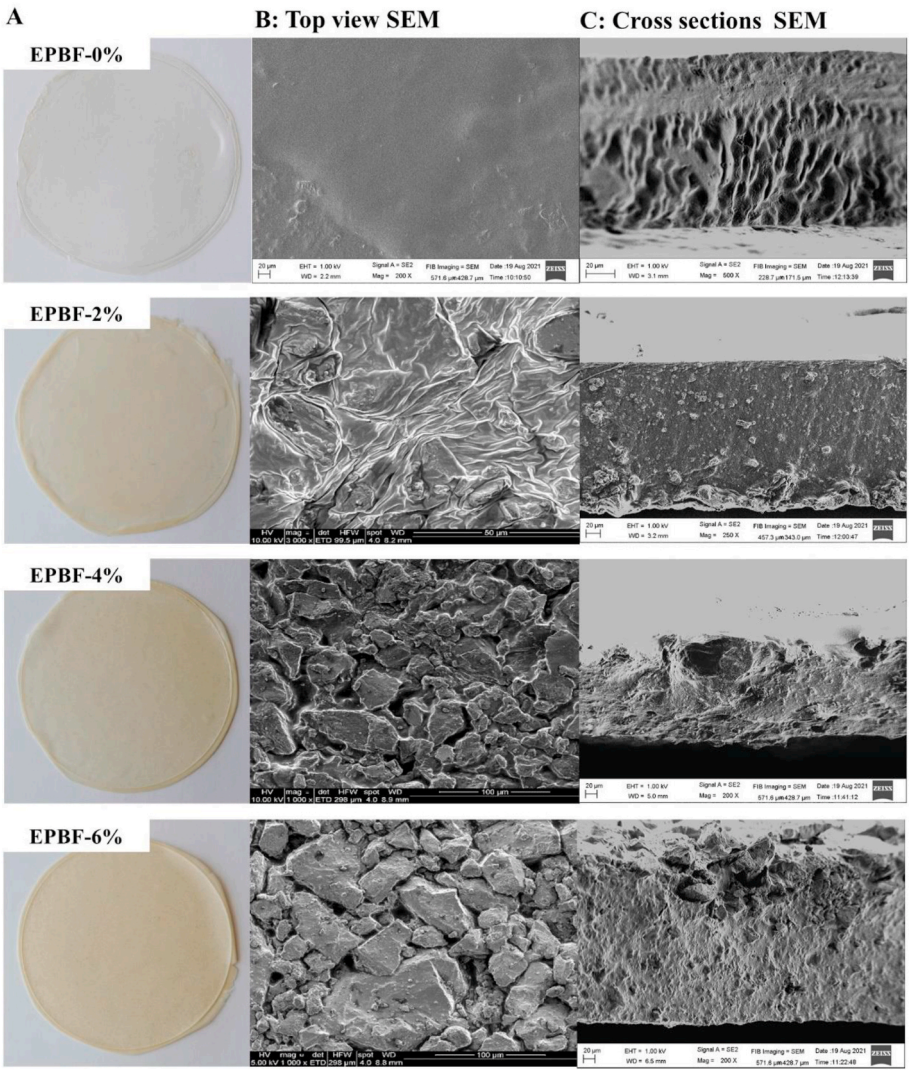

Fig. 1. Appearance (A), surface top views (B) and cross sections (C) by Scanning Electron Microscopy (SEM) of alginate/glycerol biodegradable films with different concentrations of eggshell powder of 0 (EPBF-0%), 2 (EPBF-2%), 4 (EPBF-4%) and 6% w/v (EPBF-6%).

containing EP, thus locating them in the white region of a chromaticity diagram (Valero, 2013). These results contrast with Benavides et al. (2012), who did not find significant color differences when adding synthetic calcium carbonate to alginate films. The observed differences, in addition to the origin of the ingredient (raw materials versus calcium carbonate with 99.9%), could be due do to the significantly lower concentration of calcium carbonate used in the study (0.045% w/v) compared to this study (2–6% w/v). The color of synthetic calcium carbonate is different from the color of the EP used in this work. Raw eggshells have variations in color and chemical compositions. Coloration could be relevant in the application of biodegradable films, especially when used as edible packaging; it is desirable to not change the color of foods. Interestingly, in a previous study, we observed that opaque chitosan-quinoa-oleic acid edible films, when applied by immersion in strawberries, generated a thin layer whose opacity was not detected by consumers (Valenzuela et al., 2015).

3.2.2. Mechanical properties

Mechanical properties (i.e., strength, flexibility, elongation, hardness) are critical characteristics for biodegradable films and, depending on the use, must be maintained (or not) after one or several uses. In addition, it is preferable that these films provide easy handling and storage. For example, mechanical strength is required to maintain the structural integrity of fragile contents, ideally able to prevent the biodegradable films breaking after applying accidental forces. Adequate elasticity is also desired to facilitate handling in a variety of applications, especially for food packaging (Santos et al., 2019).

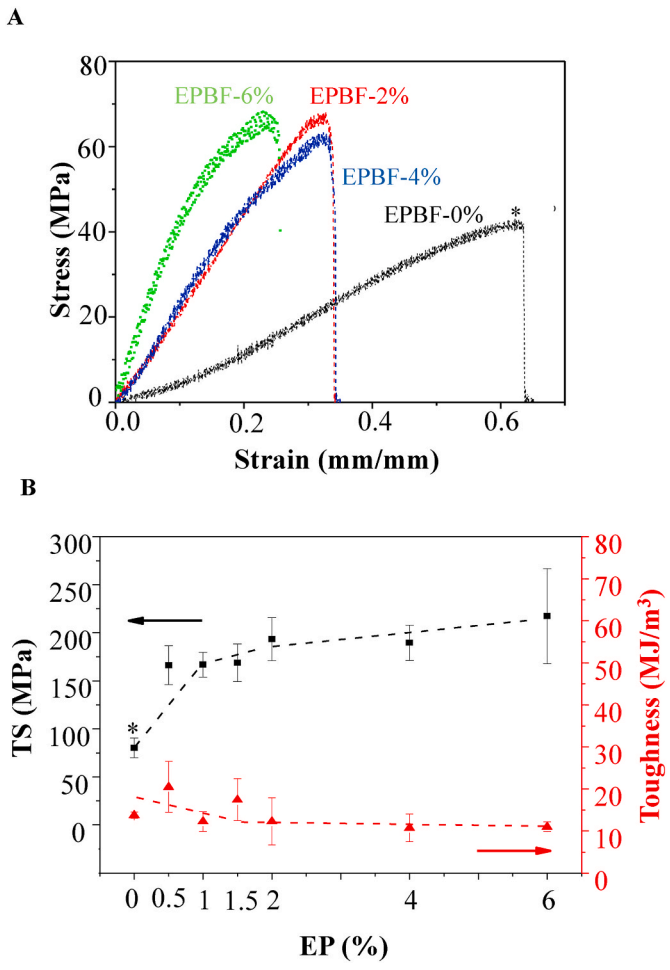

Fig. 2. A: stress-strain curves of alginate/glycerol biodegradable films with different concentrations of eggshell powder of 0 (EPBF-0%), 2 (EPBF-2%), 4 (EPBF-4%) and 6% w/v (EPBF-6%). B: tensile strength (TS) and toughness measured with different concentrations of eggshell powder (EP: 0%, 0.5%, 1%, 1.5%, 2%, 4% and 6%). *Indicates significant differences ($P < 0.05$).

A set of stress-strain curves for the EPBFs is presented in Fig. 2A. TS, EAB% and $YM_{10\%}$ values are summarized in Table 1. The EPBF-0% had the typical stress-strain curve commonly observed in other biopolymer materials with a TS of ~80 MPa (Ionita, Pandele, & Iovu, 2013; Paşcalău et al., 2012). The incorporation of EP clearly influences the mechanical properties of the EPBFs (Fig. 2A and B). Newer formulations with intermediate EP content (comprising 0.5%, 1.0% and 1.5% w/v EP) were included to provide intermediate stages of analyses and to further study the material. Even at the lowest EP content of 0.5%, the TS doubles EPBF-0%, i.e. 80 MPa *vs*. 166 MPa for EPBF-0% and EPBF-0.5%, respectively. This result, and the results from all other EPBFs, indicate that the TS parameter is very sensitive to EP content. The higher resistance to deformation created by EP is because eggshell is a tough bioceramic material (Chandan Kumar & Vasanthi, 2022; Ho, Hsu, Hsu, Hung, & Wu, 2013). Furthermore, the literature describes some specific functional groups in alginate that could bind to eggshell-derived components (such as hydroxyapatite) through Ca^{2+} ionic bonds (Sampath Kumar et al., 2014). Therefore, the concentration of guluronate residues in alginate would be key in established interactions (Browning, Stocker, Gutfreund, & Clarke, 2021); representing important applications for future work.

As shown in Fig. 2B, as EP increases, the nonlinear stress-strain characteristics gradually change to a linear one. For EPBF-2% the stress-strain curves have an elastic behavior until break (Fig. 2A). EPBF-4% are plastically deformed before rupture. Deformation becomes even more evident in EPBF-6% (Fig. 2A). The modifications of the mechanical properties due to EP incorporation into the alginate matrix are further shown in Fig. 2B where TS and toughness are plotted as a function of EP content: the higher the EP%, the harder and less tough the films become. Consistently, the reduction of toughness correlates with the increasing $YM_{10\%}$ (Table 1), meaning that the EPBFs become more brittle as the amount of EP increases. Indeed, EPBF-6% displays at least a $YM_{10\%}$ seven times larger than EPBF-0%, i.e., an average 0.05 vs. 0.35 GPa, respectively.

In terms of future applications, EPBF-2% could be applied as an edible coating on foods, where the biodegradable films must have sufficient elasticity to adhere to the contour of the food e.g. fruits such as strawberries, cherries, citrus fruits or avocado. EPBF-6% could be used as edible packaging for foods such as sausage and cheese. These formulations could also be projected for other uses, considering intermediate or even larger concentration of EP than those tested here. In addition, as the ingredients proposed for these biodegradable film formulations are edible, they could be potentially consumed with the food itself, however, a sensory panel is needed to determine consumer acceptance.

3.2.3. Microstructural properties

The optical microscopy images (Fig S1, supplementary data), showed a homogeneous and smooth surface for EPBF-0%, whereas EP particles tended to progressively agglomerate in EPBF-2%, EPBF-4% and EPBF-6%.

The superficial topography for EPBFs is shown in Fig. 1B. For EPBF-0%, a homogeneous surface was observed, corresponding to typical morphologies of alginate/glycerol films (Gong et al., 2016; Liang, Wang, & Chen, 2019). EPBF-2% presented a rough but continuous structure. A significant change occurred for EPBF-4% and EPBF-6% and is related to the presence of organized crystalloid structures, presumably from the calcium carbonate provided by EP (Fernández, Valenzuela, Arias, Neira-Carrillo, & Arias, 2016; Seifan, Samani, Hewitt, & Berenjian, 2017). Interestingly, cross sections of EPBFs show uniform structures for all formulations, indicating that calcium carbonate crystals are homogeneously distributed (Fig. 1C).

Fig. 3A shows the Field Emission Scanning Electron Microscopy (FE-SEM) images for the EPBFs, with overlayed elemental distribution

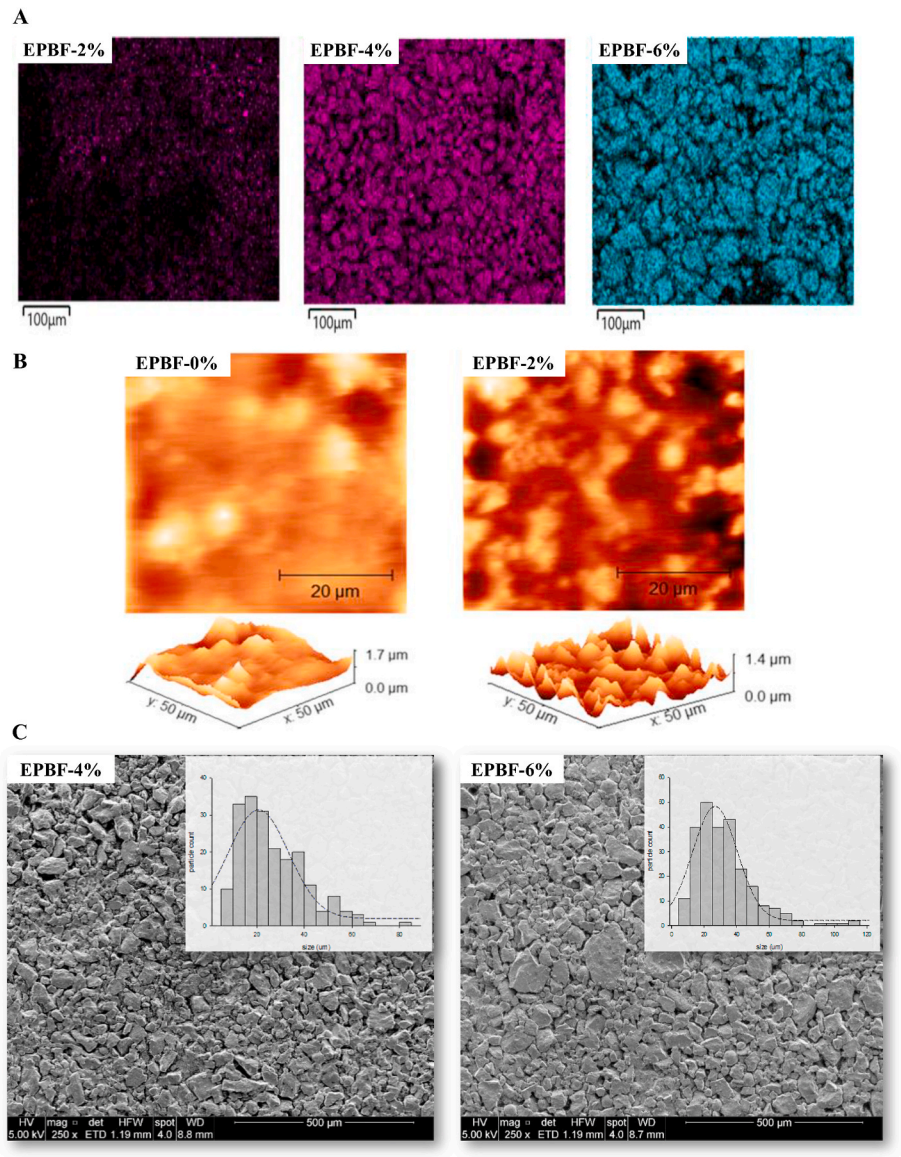

Fig. 3. A: Field Emission Scanning Electron Microscopy coupled with Energy Dispersive X-ray Spectroscopy (FE-SEM/EDX) images of calcium distribution from alginate/glycerol biodegradable films with different concentrations of eggshell powder of 2 (EPBF-2%), 4 (EPBF-4%) and 6% w/v (EPBF-6%). Calcium is shown in purple for EPBF-2%, EPBF-4% and EPBF-6%. B: AFM topological micrograph for EPBF-0% and EPBF-2% films. C: particle size distribution in the EPBF-4% and EPBF-6% films. The graphic inserted in the SEM image corresponds to the size distribution histogram of 200 particles (scale bars: 500 µm).

obtained by Energy Dispersive X-ray Spectroscopy (EDX). EPBFs were mainly composed of carbon and oxygen, which are the main atoms composing the alginate/glycerol base matrix (Saravanakumar, Sathiyaseelan, Mariadoss, Xiaowen, & Wang, 2020). As EP increased in EPBFs, the oxygen content decreased and calcium increased (Table S2, supplementary data). As expected, EPBF-0% showed no presence of calcium. EPBF-2% showed some superficial calcium, representing 1.3% of the analyzed area. EPBF-4% and EPBF-6%, show a large increase of superficial calcium (20.8% and 23.9%, respectively; see Table S2, supplementary data).

The roughness of the surface of EPBF-0% and EPBF-2% was assessed by Atomic Force Microscopy (AFM). Fig. 3B shows the topographic images with a clear increase in the surface roughness for EPBF-2%. The surface methodology response (SMR) roughness values show an increase of 60% when adding 2% EP into EPBFs (from 189 ± 9 nm for EPBF-0% to 302 ± 11 nm for EPBF-2%). EPBF-4% and EPBF-6% were too rough to be measured by this instrument. The higher roughness observed is explained by the pattern that EP particles give to EPBF-4% and EPBF-6%, when organized as a "grain structure" (Fig. 3C), composed mainly of calcium atoms (Fig. 3A).

Key microstructural properties of films such as porosity and particle distribution were analyzed. It is interesting to note that the EPBFs were not porous, showing porosity values below 300 nm, and a specific surface area (S_{BET}) close to 0 m^2/g. This agrees with the pore volume obtained from the CO_2 isotherm values (ranging from 0.000574 to 0.001573 cm^3/g). The low porosity of EPBFs could be explained because the predominant $CaCO_3$ form in eggshell is calcite (Aigbodion & Akinlabi, 2019; Atikpo, Aigbodion, & Von Kallon, 2022), which is the most stable and least porous (Achour et al., 2017).

The particle distribution in the EPBFs was also studied. Fig. 3C shows that particles in EPBF-4% and EPBF-6% are clustered as organized grain structures with size particle distribution peaks of 20.7 ± 2.0 and 26.6 ± 1.1 µm, respectively. The EPBF-2% particles were heterogeneously dispersed, providing low numbers of particles to be counted, which prevented a distribution peak analysis in a similar area as the others EPBFs. The study of the particle size, as well as their distribution in the EPBFs, is of interest because of its impact on the film microstructure and physical properties, such as water vapour permeability, mechanical properties, and general barrier properties (Jiménez, Fabra, Talens, & Chiralt, 2010).

The study of surface morphology and topographical characteristics of the EPBFs is very important for their application, since it has been described that highly heterogeneous, rough and porous film surfaces could generate materials with: i) very low fracture toughness, and ii) low

adhesiveness and moldability (Jouki, Khazaei, Ghasemlou, & Hadi-Nezhad, 2013; Valenzuela et al., 2013, 2015). Low fracture toughness is one of the most complex characteristic to reproduce in biodegradable films compared to plastics materials. Low adhesiveness and moldability is important for adhesion of films to food contours for their use as coating or to develop functional packaging. Other authors have reported that the use of $CaCO_3$ in coating formulations led to materials with very low strength and impact resistance, and with moderate moldability (Lucas, Borrajo, & Williams, 1993; Osman, Atallah, & Suter, 2004). However, in this study it was observed that the use of EP (which is mainly composed of $CaCO_3$), improved the tensile strength of the films, as discussed in section 3.2.2. Based on the results obtained, we hypothesize that the EP particles form a rough monolithic layer, which has very low porosity and is structurally cohesive with the polymer matrix explaining the improvements in mechanical properties; which could be influenced by the contribution of protein from the shell membranes and traces of albumin contained in the egg shells used in this study. The proteins could act as surfactants, which have been shown to improve the properties of $CaCO_3$- polymeric coatings due to a good compatibility and strong interaction between proteins and $CaCO_3$ (Barhoum et al., 2014; Bastrzyk, Fiedot-Tobola, Polowczyk, Legawiec, & Płaza, 2019; Fu, Qiu, Orme, Morse, & De Yoreo, 2005; Liu et al., 2008).

3.2.4. Powder X-ray diffraction (PXRD) and 2D wide angle X-ray scattering (2D WAXS)

X-ray diffraction is a technique used for determining atomic structure. It provides information on sample crystallinity, via diffractograms, distinguishing between amorphous and crystalline states that could predict the material behavior in future applications. Table S1 (supplementary data) displays the 2θ values, observed and calculated, with the corresponding relative intensity as well as the observed and calculated d values using Bragg's law for the EP as well as EPBF samples. Miller indexes were determined by refinement using WinXPOW INDEX Version 2.03 (STOE GmbH). Powder X-ray diffraction assay is shown in Fig. 4. The results show that EP is primarily composed of trigonal calcite, in the space group R-3 c, in agreement with literature for most avian eggshells (Cahya & Marfuah, 2014; Nys, Gautron, Garcia-Ruiz, & Hincke, 2004; Spelta & Galdino, 2018). The refined cell parameters are a = b = 4.9869 and c = 17.0526.

Both PXRD and WAXS patterns show the scattering of the polymeric matrix together with the diffraction pattern of the EP. The eggshell diffraction patterns in the EPBF samples are the same as the neat eggshell powder (EP, calcite phase), without any modification in cell parameters, which means that it does not undergo any chemical modification within the resolution of the XRD measurements. The control matrix (EPBF-0%) shows an amorphous phase with diffuse scattering patterns, which implies that the sodium alginate/glycerol system does not yield any structuration at the molecular scale.

Natural calcite exists in the sample as discrete crystals, as seen in the 2D WAXS measurements (Fig S2, supplementary data) The 2D WAXS pattern shows spotty diffraction patterns according to the calcite phase.

We used WAXS measurements to assess the $CaCO_3$ content (as the main component of EP) in the EPBFs. The area of the (0 1 2) diffraction peak was chosen to normalize the lowest concentration of EPBF-2% (18.0%). We estimated a $CaCO_3$ content of 32.0% and 50.3% in the EPBF-4% and EPBF-6%, respectively. Since the X-ray is always perpendicular to the film plane, preferential orientation of the eggshell particles cannot be ruled out. These values are quite distant from those found by FE-SEM/EDX (see Table S2., supplementary data), since this technique records the surface concentration of EP in EPBFs. This agrees with the SEM photographs (cross section) (Fig. 1C), where it is observed that for samples with increasing EP loading (EPBF-4% and EPBF-6%), the polymeric mixture goes to the bottom in the casting process, leaving more EP exposed on the surface.

According to the data presented for PXRD and WAXS, all EPBFs were notably amorphous. As far as we know, the amorphous domains that conform the films have greater susceptibility to compression and decompression processes, favoring changes in the structures, and consequently on the mechanical properties of the EPBFs. Furthermore, its amorphous structure promotes EPBFs solubility in water (Choi et al., 2022). Since amorphous materials are more feasibly to absorbe surrounding water, water will act as a plastizicer, decreasing the glass transition temperature (Tg) and potentially affecting the storage stability (Espíndola, Norder, Koper, & Picken, 2023).

3.2.5. Fourier Transform Infrared Spectroscopy (FTIR)

The FTIR spectroscopy was performed to obtain reliable information about the chemical composition and the possible interactions between components in the EPBFs that could include the formation of new functional groups and/or destabilization of the components (Castro-Yobal et al., 2021; Gieroba et al., 2020; Luo et al., 2019). In our investigation, FTIR was used to analyze the EP and EPBFs (Fig. 5). In EP the characteristic bands of calcium carbonate were observed in the IR spectrum at 710, 871 and 1410 cm^{-1} (Guru & Dash, 2014; Naemchan, Meejoo, Onreabroy, & Limsuwan, 2008). The band at 710 cm^{-1} corresponds to the bending of the C–O group of calcium carbonate (Abdel-Khalek, Abdel Rahman, & Francis, 2017). The bands at 871 and 1410 cm^{-1} correspond to asymmetric stretching of CO_3^{-2} molecules (Awogbemi, Inambao, & Onuh, 2020; Clark, 1995; Jazie, Sinha, & Pramanik, 2013). The band at 2360 cm^{-1} present in EP and all EPBFs corresponds to the asymmetric stretching vibration of CO_2 (Liu, Cai, Ma, Sheng, & Huang, 2020; Pasquali, Andanson, Kazarian, & Bettini, 2008; Zhang et al., 2018).

In the EPBFs, the spectra are similar and present absorption bands in

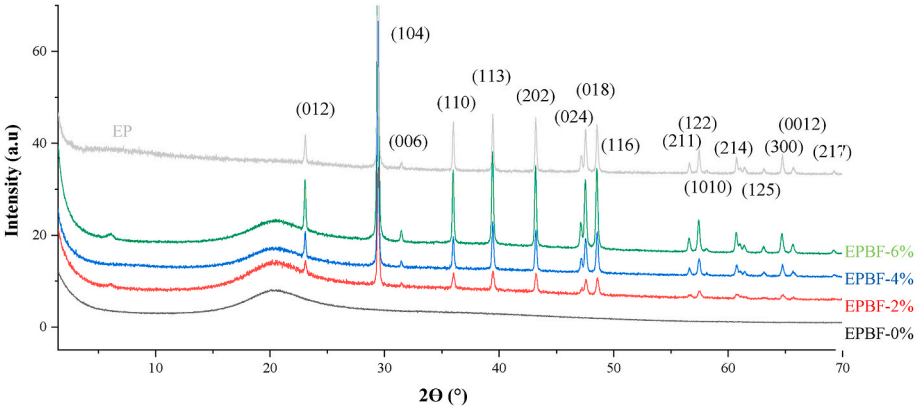

Fig. 4. Powder x-ray diffraction (PXRD) for eggshell powder (EP) and alginate/glycerol biodegradable films (EPBFs) with different concentrations of eggshell powder: 0 (EPBF-0%), 2 (EPBF -2%), 4 (EPBF -4%) and 6% w/v (EPBF -6%).

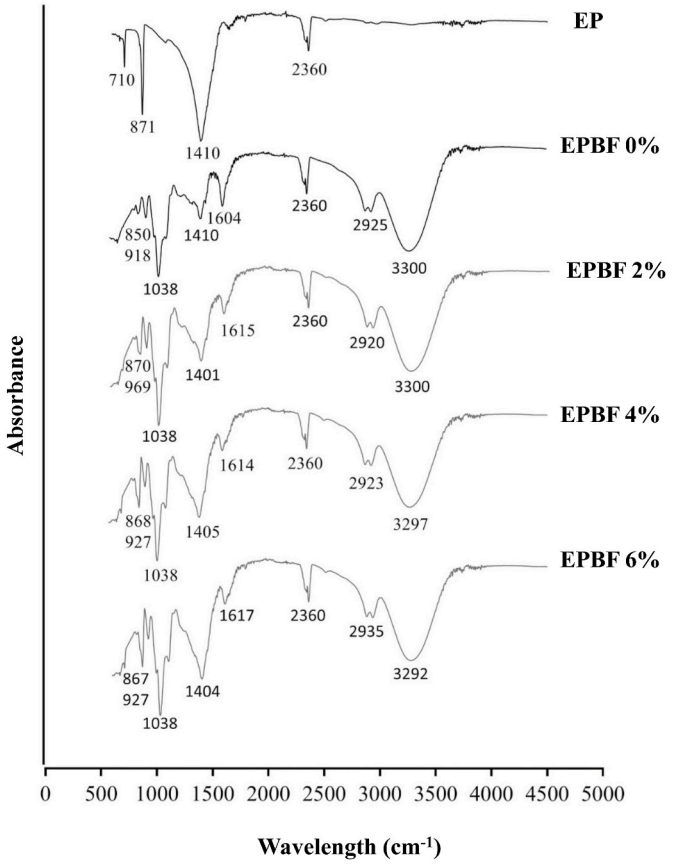

Fig. 5. Fourier Transform Infrared Spectroscopy of eggshell powder (EP) and alginate/glycerol biodegradable films (EPBFs) with different concentrations of eggshell powder of 0 (EPBF-0%), 2 (EPBF-2%), 4 (EPBF-4%) and 6% w/v (EPBF-6%).

the same regions with some slight differences. The absorption bands near 860 cm^{-1} are related to the C–H bond of the glucuronic acid in alginate (Mahcene et al., 2020). The band at 1038 cm^{-1} corresponds to the bending vibration of the O–H group of alginate, due to the formation of hydrogen bonds with water (Xiao, Gu, & Tan, 2014). The region close to 1400 cm^{-1} and 1600 cm^{-1} indicate symmetric and asymmetric stretching vibrations of the COO^{-} group due to the presence of uronic acid in alginate (Lawrie et al., 2007; Mahcene et al., 2020; Xiao et al., 2014). The band of 1400 cm^{-1} also corresponds to the stretching of the C–O group of carbonate provided by EP (Prapruddivongs & Wongpreedee, 2020), explaining why this band is more prominent in EPBFs with higher EP concentrations. The peaks around 2930 cm^{-1} were attributed to C–H stretching vibration (Li et al., 2021; Nordin, Othman, Rashid, & Basha, 2020; Teixeira et al., 2021). Glycerol is an alcohol with a chemical structure containing CH groups, so its incorporation into films may have caused an increase in the interactions between the compounds in that region of the band (Gonçalves et al., 2019). The 3300 cm^{-1} band corresponds to the stretching of the O–H group (Lawrie et al., 2007), this band is explained by the formation of hydrogen bridges between alginate and glycerol due to the uptake of water molecules and subsequent hydration. It is important to note, that those bands observed around 1400 cm^{-1}, 1600 cm^{-1}, 2900 cm^{-1} and 3300 cm^{-1} exhibit a slight shift from the EP and EPBF-0% to the EPBFs (2%, 4%, 6%), which is indicative of the interaction between the EP and the alginate/glycerol (Luo et al., 2019). Previous studies indicate that changes on the band position, that are related to the formation of hydrogen bonds between the components, could induce stronger intramolecular interactions improving the physical and mechanical properties of the biodegradable films (Luo et al., 2019; Tongdeesoontorn, Mauer, Wongruong, Sriburi, & Rachtanapun, 2011).

3.2.6. Thermal characterization (MDSC, TGA)

MDSC curves of EPBF-6% in non-hermetic pan under N_2 shows the dehydration process by a broad endothermic peak centered at 65 °C, in the range 10 °C–110 °C. Afterwards the decomposition of the biopolymer takes place at c.a. 170 °C–220 °C, represented by an endotherm peak. In this step, there is an important evolution of glycerol, as was observed in the heating stage. The behavior in this zone is different from what observed in literature (Soares, Santos, Chierice, & Cavalheiro, 2004). While they find an exothermal decomposition, in this study endothermic peak is seen due to the evaporation of the excess of glycerol. Finally, a decrease in the Cp above 270 °C showed the final decomposition of the carbonaceous material (Fig. 6A).

For hermetic pans, we observed 4 transitions for all samples. At 143 °C and 159 °C, two small endothermic events which could be understood as melting of two low molecular weight fractions of alginate. Then a broad exothermic peak centered at c.a. 173 °C and a sharp peak around 190 °C, which are decomposition processes of alginate and glycerol under the pan internal pressure. For process 4, EPBF-6% shows the decomposition at lower temperatures due to the excess of EP ($CaCO_3$), which must be overheating the surrounding organic material (Fig. 6B).

The EPBFs have a similar TG measurement in a nitrogen atmosphere as the calorimetric curves (Fig. 6C). While we see 3 major decomposition steps, (proc 1 to 3 and 6) the differential curves (DTG) show further mass loss events (Fig. 6D). Initial weight loss up to 150 °C is due to the moisture loss from the sample (Proc. 1). Concurrent polymer degradation and glycerol evolution as a main weight loss is seen in the second stage between 150 °C and 310 °C (Proc. 2 and 3 respectively). Two minor events in the ranges 330 °C–390 °C and 390 °C–500 °C (Proc. 4 and 5) were observed, attributed to further decomposition of organic residues, leaving just $CaCO_3$ and Na_2CO_3. A step between 600 °C and 800 °C must be due to the $CaCO_3$ decomposition to CaO (Proc. 6). The transformation of Na_2CO_3 to Na_2O is detected in EPBF-0% between 710 °C and 750 °C which is hidden under the bigger Proc. 6 in the EP containing samples (Zhao et al., 2010).

In general, the thermal analysis showed several thermal processes. The thermal behavior did not change abruptly at low EP concentrations in EPBFs. Only for EPBF-6% was a noticeable change observed, with a decrease in the decomposition temperature in sealed pans. According to our experience, the inorganic component of EP could transfer more efficiently the thermal energy to the whole material and negatively influencing the decomposition. However, these changes occur at high temperatures, therefore, it would not affect its application as a coating on foods that are kept under refrigeration or room temperature. On the other hand, if EPBFs were used as edible films on foods that are cooked at high temperatures, they would degrade progressively. This thermal behavior is typical of composite materials, where both organic (alginate/glycerol) – inorganic ($CaCO_3$) constituents behave as such separately.

3.2.7. Biodegradability properties

Thewettability of biomaterials is a prerequisite for projecting desired responses, such as degradation rates. It corresponds to the ease for spreading of liquid on the surface, which is directly related to the intermolecular forces between the phases. This behaviour is commonly estimated by contact angle measurements (hydrophilicity $<90° <$ hydrophobicity) (Agrawal, Negi, Pradhan, Dash, & Samal, 2017; Grainger & Castner, 2017). As shown in Table 1, the contact angle values obtained for EPBFs increase with increasing EP concentration (27.4° for EPBF-0% to 62.3° for EPBF-6%). These results demonstrate the role of EP in decreasing the hydrophilicity of EPBFs, due to the presence of calcite in EP, which is the most insoluble form of calcium carbonate (Akin & Lagerwerff, 1965).

To complement the hydrophilicity results of EPBFs, hydrosolubility

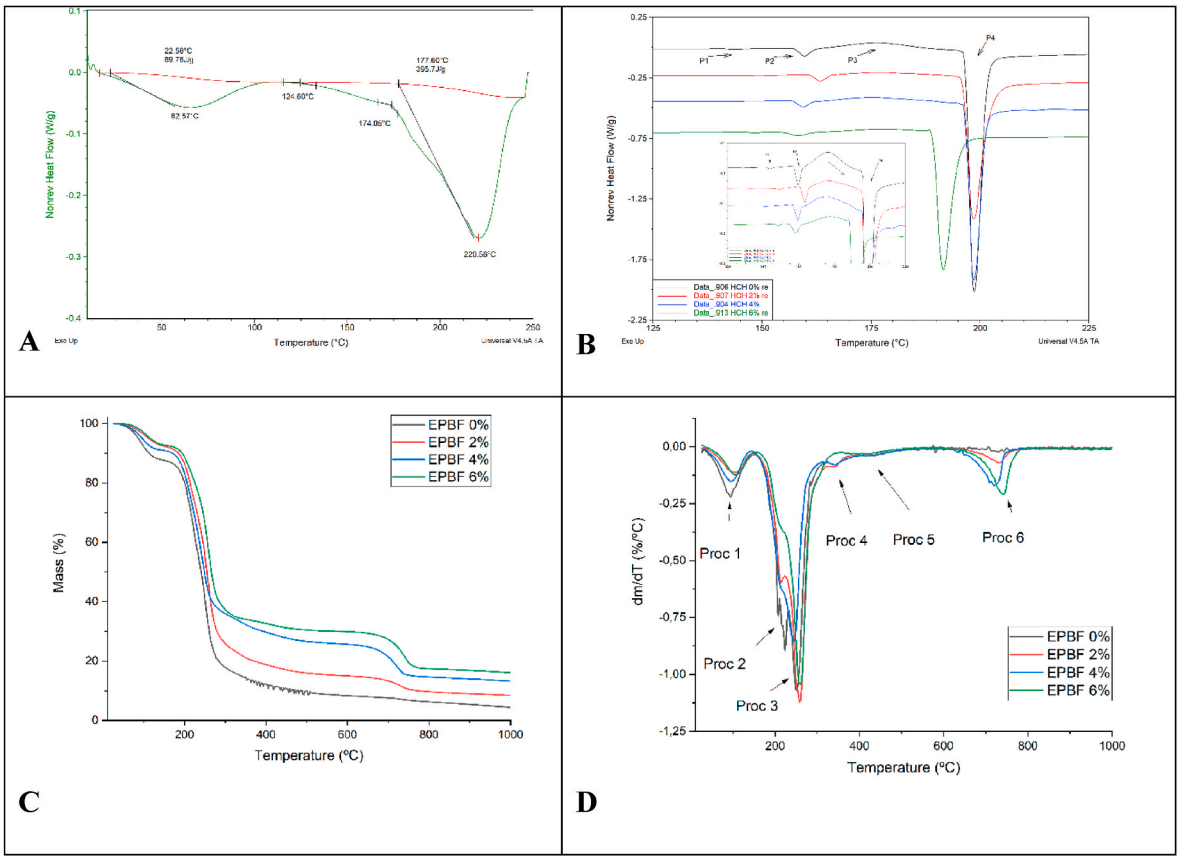

Fig. 6. (A) Modulated Differential Scanning Calorimetry (MDSC) curves of EPBF-6% in non-hermetic pan under N_2. (B) MDSC non-reversible traces for EPBF-0%, EPBF-2, EPBF-4 and EPBF-6%. (C) Thermogravimetric Analysis (TGA) and (D) differential thermogravimetry (DTG) of the investigated samples.

assays were also performed. The solubility percentages are shown in Table 1. As expected, EPBF-0% had a significantly higher solubility than formulations with increasing EP, although solubility for all EPBFs was high. The high solubility of EPBF-0% is explained by the hydrophilic nature of its constituent (alginate and glycerol), especially glycerol, that favors the absorption of water molecules (Mei, Yuan, Wu, & Li, 2013). Meanwhile, the incorporation of EP generated a decrease in the solubility of the EPBFs as explained above. Interestingly, contact angle values of the EPBF-4% and EPBF-6% were about 2.7 times greater than EPBF-0% and EPBF-2% (Table 1), indicating that the former are more hydrophobic. However, water solubility values did not change between EPBF-2% and EPBF-4%, as found for contact angle values. This could be due to the surficial hydrophobicity of EPBF-4% and EPBF-6%. Similar results for contact angle and solubility values were found by Abdollahi et al. (2013) using cellulose nanocrystals as alginate film reinforcement. Solubility of films decreased consistently with increasing content of cellulose nanocrystals (until 5%), but contact angle values increased suddenly between 0 and 1% of cellulose nanocrystals, because of their hydrophobic nature.

One of the major concerns regarding plastic waste is its impact on the environment. In addition to possible toxic effects generated by microplastics, which can accumulate in soil and water, affecting plant and animal species (Salimi, Alavehzadeh, Ramezani, & Pourahmad, 2022; Yuan, Nag, & Cummins, 2022). Therefore, the development of a material capable of degrading completely in a short time represents an enormous environmental advantage. Fig. 7A shows the weight loss of the EPBFs at different times under vermicomposting. In the first stage (7 days), a slow degradation process was observed with an initial weight loss between 10% and 30%. In the second stage (14 days), faster degradation was observed with a weight loss of ≈80% (EPBF-6% showed complete degradation). At 21 days, the residual structures were completely degraded (with the exception of EPBF-0%). Fig. 7B shows physical changes after biodegradation of EPBF-0% and EPBF-6% in the vermicomposting system. On day 7, all the EPBFs had started the degradation process, presenting a rough appearance and changes in coloration. EPBF-0% and EPBF-2% remained almost whole, while EPBF-4% y EPBF-6% are fragmented. On day 14, EPBF-6% was completely degraded (Fig. 7B and Video 2, supplementary data) whereas fragments were observed for other EPBFs (0–4%). At day 21, only fragments of EPBF-0% were found. Importantly, the velocity of degradation was higher in this study compared to other authors. For example, Bandyopadhyay et al. (2019), did not obtain 100% degradation in 28 days for biodegradable films composed of bacterial cellulose and guar gum. Bootklad and Kaewtatip (2013) developed thermoplastic starch/eggshell powder composites, which did not completely biodegrade after 15 days. Tang, Zou, Xiong, and Tang (2008) developed starch/polyvinyl alcohol/nano-silicon dioxide biodegradable films that did not completely biodegrade until 120 days. In this regard, the organic compounds in EP (i.e. proteins) could make the EPBFs more attractive to earthworms, in addition EP could also be significantly more susceptible to biodegradation by microorganisms in the vermicomposting ecosystem (Bootklad & Kaewtatip, 2013).

Several aspects of the potential applications of EPBFs as biodegradable coatings or packaging are described in this work based on the nature of the components, microstructure of the films, chemical interactions and biodegradability properties. Forthis study, we highlight the “grain structure” observed in Fig. 3C. This structure could act as a physical barrier hindering the penetration of water molecules into the EPBFs. This property is relevant when considering the application of these biodegradable films in foods with high respiration rates and the generation of water vapour, such as climacteric fruits and vegetables (Castellanos, Herrera, & Herrera, 2016; Garavito, Herrera, &

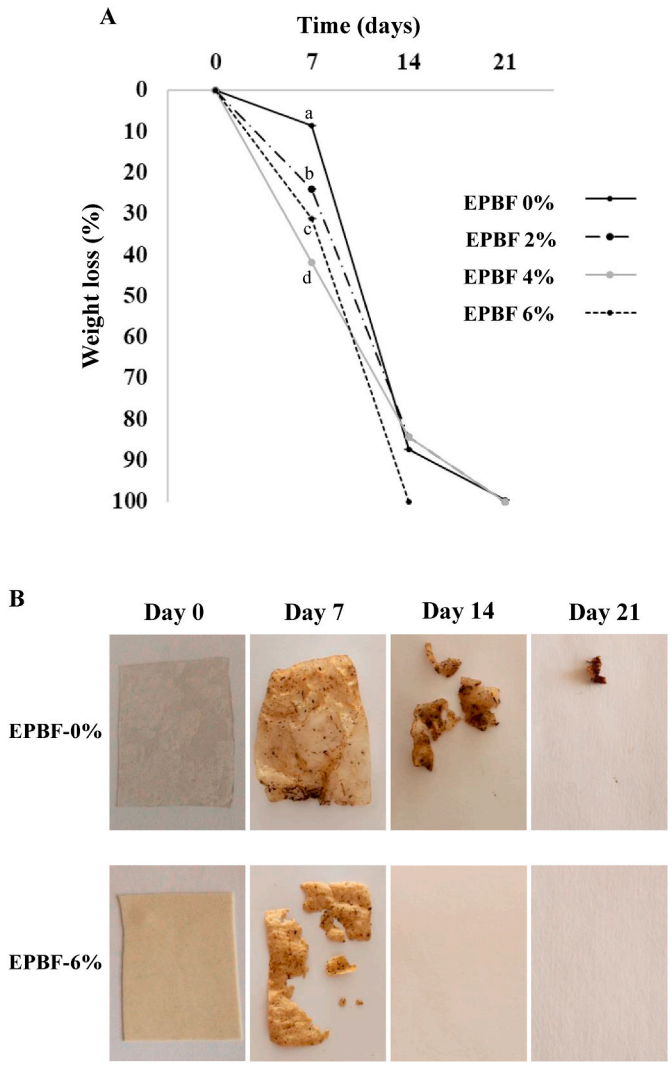

Fig. 7. (A) Weight loss of alginate/glycerol biodegradable films with different concentrations of eggshell powder of 0 (EPBF-0%), 2 (EPBF-2%), 4 (EPBF-4%) and 6% w/v (EPBF-6%), after biodegradability test in vermicomposting. (B) Appearance of EPBF-0% and EPBF-6% after of biodegradability test in vermicomposting. Different letters indicate significant differences ($P < 0.05$).

Castellanos, 2021). The solubilization assay showed the EPBFs fracture into several fragments after 1 h, gradually decreasing in size. This test indicates that EPBFs could be reduced at the household level by simply immersing them in water. Unlike petroleum-derived plastics, EPBFs do not generate microplastics, since their dissolution generates residues containing non-accumulating elements from sodium alginate, glycerol and eggshell. They are biocompatible, biodegradable and non-toxic compounds. Furthermore, alginate, glycerol and calcium carbonate have been used in soil fertilizers (Arafa, Sabaa, Mohamed, Elzanaty, & Abdel-Gawad, 2022; Borges, Soares Giroto, Klaic, Wypych, & Ribeiro, 2021). EP could also be useful as a compostable ingredient (Aditya, Stephen, & Radhakrishnan, 2021). As discussed, our formulations degrade by vermicomposting faster compared to other studies. (Bootklad & Kaewtatip, 2013).

The need to obtain water-soluble and vermicompostable film depends on the intended application (Pelissari, Andrade-Mahecha, Sobral, & Menegalli, 2013). Water-solubility is convenient for future applications as edible packaging for coffee, instant soup, dehydrated puree. For example, coffee packaging that is capable of dissolving in hot water. EPBFs could also be used as calcium vehicles, since calcium carbonate is the most widely used calcium salt for fortification and supplementation strategies (Masuda & Hiramatsu, 2007; Schaafsma et al., 2000).

4. Conclusions

In this research, biodegradable and vemicompostable alginate/glycerol and eggshell powder based films were developed by a simple and low-cost method. The EPBFs were whitish and opaque in appearance, showed heterogeneous, rough microstructure and low porosity. The eggshell particles were distributed in a monolithic pattern on the polymeric matrix, where interactions were established, possibly between EP functional groups, shell membrane proteins and traces of albumin and matrix functional groups. These interactions, together with the firmness provided by EP as a bioceramic, improved mechanical properties, producing films that were more resistant to fracture. The EP content also significantly increased the hydrophobicity of the EPBFs. Importantly, the films are biodegradable in water and can be disposed of at home and completely biodegrade under vermicomposting in short periods of time (between 14 and 21 days). EPBFs obtained from waste constitute a potential alternative as a coating or packaging that does not generate environmental pollution.

Funding

This research did not receive any specific grant from funding agencies in the public, commercial, or not-for-profit sectors.

Credit author statement

Valeria Villanueva: Methodology, Validation, Formal analysis, Investigation, Writing – original draft preparation, Writing – review and editing, Visualization. Fabrizzio Valdés: Investigation, Writing – review and editing, Visualization. Rommy N. Zúñiga: Methodology, Validation, Formal analysis, Investigation. María Gabriela Villamizar-Sarmiento: Investigation, Writing – review and editing. Eduardo Soto-Bustamante: Methodology, Validation, Formal analysis, Investigation. Patricio Romero-Hasler: Methodology, Validation, Formal analysis. Jose Tapia: Methodology, Validation, Formal analysis. Judit Lisoni: Methodology, Validation, Formal analysis, Investigation. Felipe Oyarzun-Ampuero: Investigation, Writing – review and editing, Visualization. Carolina Valenzuela: Conceptualization, Methodology, Validation, Formal analysis, Investigation, Resources, Writing – original draft preparation, Writing – review and editing, Visualization, Supervision, Project administration.

Declaration of competing interest

The authors declare that they have no known competing financial interests or personal relationships that could have appeared to influence the work reported in this paper.

Data availability

Data will be made available on request.

Acknowledgments

JL thanks the *Unidad de Microscopía Electronica* core facility of Universidad Austral de Chile, a Zeiss Reference Center for Latin-American, for the use of the FESEM Auriga system. CV and FO thanks to EQM170111, EDS detector of FE-SEM (Inspect F50), Facultad de Ciencias Químicas y Farmacéuticas, Universidad de Chile. ES and FO thanks to FONDEQUIP EQM 200266 and ANID/PIA/ACT192144. FO thanks to CONICYT-FONDAP 15130011. The authors gratefully acknowledge Susan Cleveland for assistance in reviewing the English in this manuscript.

Appendix A. Supplementary data

Supplementary data to this article can be found online at https://doi.org/10.1016/j.foodhyd.2023.108813.

References

Abdel-Khalek, M. A., Abdel Rahman, M. K., & Francis, A. A. (2017). Exploring the adsorption behavior of cationic and anionic dyes on industrial waste shells of egg. *Journal of Environmental Chemical Engineering, 5*(1), 319–327. https://doi.org/10.1016/j.jece.2016.11.043

Abdollahi, M., Alboofetileh, M., Rezaei, M., & Behrooz, R. (2013). Comparing physico-mechanical and thermal properties of alginate nanocomposite films reinforced with organic and/or inorganic nanofillers. *Food Hydrocolloids, 32*(2), 416–424. https://doi.org/10.1016/j.foodhyd.2013.02.006

Abera, G., Woldeyes, B., Demash, H. D., & Miyake, G. (2020). The effect of plasticizers on thermoplastic starch films developed from the indigenous Ethiopian tuber crop Anchote (*Coccinia abyssinica*) starch. *International Journal of Biological Macromolecules, 155*, 581–587. https://doi.org/10.1016/j.ijbiomac.2020.03.218

Achour, A., Arman, A., Islam, M., Zavarian, A. A., Basim Al-Zubaidi, A., & Szade, J. (2017). Synthesis and characterization of porous $CaCO_3$ micro/nano-particles. *The European Physical Journal Plus, 132*(6), 267. https://doi.org/10.1140/epjp/i2017-11531-8

Aditya, S., Stephen, J., & Radhakrishnan, M. (2021). Utilization of eggshell waste in calcium-fortified foods and other industrial applications: A review. *Trends in Food Science & Technology, 115*, 422–432. https://doi.org/10.1016/j.tifs.2021.06.047

Agrawal, G., Negi, Y. S., Pradhan, S., Dash, M., & Samal, S. K. (2017). Wettability and contact angle of polymeric biomaterials. In M. C. Tanzi, & S. Farè (Eds.), *Characterization of polymeric biomaterials* (pp. 57–81). Elsevier. https://doi.org/10.1016/B978-0-08-100737-2.00003-0.

Agrawal, N., Thakur, O. P., & Singh, A. K. (2021). Role of shape, size and concentration of filler particles on filler matrix interface: A mathematical analysis. *Materials Today: Proceedings, 44*, 890–894. https://doi.org/10.1016/j.matpr.2020.10.793

Aigbodion, V. S., & Akinlabi, E. T. (2019). Explicit microstructural evolution and electrochemical performance of zinc-eggshell particles composite coating on mild steel. *Surfaces and Interfaces*. , Article 100387. https://doi.org/10.1016/j.surfin.2019.100387

Akin, G. W., & Lagerwerff, J. V. (1965). Calcium carbonate equilibria in solutions open to the air. II. Enhanced solubility of $CaCO_3$ in the presence of Mg^{2+} and SO_4^{2-}. *Geochimica et Cosmochimica Acta, 29*(4), 353–360. https://doi.org/10.1016/0016-7037(65)90026-8

Al-awwal, N. Y., & Ali, U. L. (2015). Proximate analyses of different samples of egg shells obtained from Sokoto market in Nigeria. *International Journal of Science and Research, 4*(3), 564–566. https://doi.org/10.21275/sub152011

Al-Salem, S. M., Lettieri, P., & Baeyens, J. (2009). Recycling and recovery routes of plastic solid waste (PSW): A review. *Waste Management, 29*(10), 2625–2643. https://doi.org/10.1016/j.wasman.2009.06.004

Alshehrei, F., & Ameen, F. (2021). Vermicomposting: A management tool to mitigate solid waste. *Saudi Journal of Biological Sciences, 28*(6), 3284–3293. https://doi.org/10.1016/j.sjbs.2021.02.072

AOAC Association of Official Analytical Chemists. (1996). *Official methods of analysis of AOAC international* (16th ed.). Arlington, USA: AOAC International.

Arafa, E. G., Sabaa, M. W., Mohamed, R. R., Elzanaty, A. M., & Abdel-Gawad, O. F. (2022). Preparation of biodegradable sodium alginate/carboxymethylchitosan hydrogels for the slow-release of urea fertilizer and their antimicrobial activity. *Reactive and Functional Polymers, 174*, Article 105243. https://doi.org/10.1016/j.reactfunctpolym.2022.105243

Atikpo, E., Aigbodion, V. S., & Von Kallon, D. V. (2022). $CaCO_3$-derived from eggshell waste for improving the corrosion resistance of zinc composite coating on mild steel for biodiesel storage tank. *Chemical Data Collections, 37*, Article 100794. https://doi.org/10.1016/j.cdc.2021.100794

Avella, M., Di Pace, E., Immirzi, B., Impallomeni, G., Malinconico, M., & Santagata, G. (2007). Addition of glycerol plasticizer to seaweeds derived alginates: Influence of microstructure on chemical–physical properties. *Carbohydrate Polymers, 69*(3), 503–511. https://doi.org/10.1016/j.carbpol.2007.01.011

Awogbemi, O., Inambao, F., & Onuh, E. I. (2020). Modification and characterization of chicken eggshell for possible catalytic applications. *Heliyon, 6*(10), Article e05283. https://doi.org/10.1016/j.heliyon.2020.e05283

Bandyopadhyay, S., Saha, N., Brodnjak, U. V., & Sáha, P. (2019). Bacterial cellulose and guar gum based modified PVP-CMC hydrogel films: Characterized for packaging fresh berries. *Food Packaging and Shelf Life, 22*, Article 100402. https://doi.org/10.1016/j.fpsl.2019.100402

Barhoum, A., Rahier, H., Abou-Zaied, R. E., Rehan, M., Dufour, T., Hill, G., et al. (2014). Effect of cationic and anionic surfactants on the application of calcium carbonate nanoparticles in paper coating. *ACS Applied Materials & Interfaces, 6*(4), 2734–2744. https://doi.org/10.1021/am405278j

Barnes, D. K. A. (2002). Invasions by marine life on plastic debris. *Nature, 416*, 808–809. https://doi.org/10.1038/416808a

Bastrzyk, A., Fiedot-Toboła, M., Polowczyk, I., Legawiec, K., & Płaza, G. (2019). Effect of a lipopeptide biosurfactant on the precipitation of calcium carbonate. *Colloids and Surfaces B: Biointerfaces, 174*, 145–152. https://doi.org/10.1016/j.colsurfb.2018.11.009

Benavides, S., Villalobos-Carvajal, R., & Reyes, J. E. (2012). Physical, mechanical and antibacterial properties of alginate film: Effect of the crosslinking degree and oregano essential oil concentration. *Journal of Food Engineering, 110*(2), 232–239. https://doi.org/10.1016/j.jfoodeng.2011.05.023

Bhat, S. A., Singh, S., Singh, J., Kumar, S., Bhawana, & Vig, A. P. (2018). Bioremediation and detoxification of industrial wastes by earthworms: Vermicompost as powerful crop nutrient in sustainable agriculture. *Bioresource Technology, 252*, 172–179. https://doi.org/10.1016/j.biortech.2018.01.003

Bonilla, J., & Sobral, P. J. A. (2020). Disintegrability under composting conditions of films based on gelatin, chitosan and/or sodium caseinate containing boldo-of-Chile leafs extract. *International Journal of Biological Macromolecules, 151*, 178–185. https://doi.org/10.1016/j.ijbiomac.2020.02.051

Bootklad, M., & Kaewtatip, K. (2013). Biodegradation of thermoplastic starch/eggshell powder composites. *Carbohydrate Polymers, 97*(2), 315–320. https://doi.org/10.1016/j.carbpol.2013.05.030

Borges, R., Soares Giroto, A., Klaic, R., Wypych, F., & Ribeiro, C. (2021). Mechanochemical synthesis of eco-friendly fertilizer from eggshell (calcite) and KH_2PO_4. *Advanced Powder Technology, 32*(11), 4070–4077. https://doi.org/10.1016/j.apt.2021.09.013

Browning, K. L., Stocker, I. N., Gutfreund, P., & Clarke, S. M. (2021). The effect of alginate composition on adsorption to calcium carbonate surfaces. *Journal of Colloid and Interface Science, 581*, 682–689. https://doi.org/10.1016/j.jcis.2020.07.088

Brunauer, P. H., Emmett, E., & Teller, E. (1938). Adsorption of gases in multimolecular layers. *Journal of the American Chemical Society, 60*, 309–319. https://doi.org/10.1021/ja01269a023

Cahya, M., & Marfuah, N. (2014). Identification of calcium carbonate ($CaCO_3$) characteristics from different kinds of poultry eggshells using x-ray diffraction (XRD) and Fourier transformation infra-red (FTIR). *Proceedings of the 2014 International Conference on Physics and Its Applications, 1*, 138–142. https://doi.org/10.2991/icopia-14.2015.27

Campbell, L., Raikos, V., & Euston, S. R. (2003). Modification of functional properties of egg-white proteins. *Nahrung-Food, 47*(6), 369–376. https://doi.org/10.1002/food.200390084

Castellanos, D. A., Herrera, D. R., & Herrera, A. O. (2016). Modelling water vapour transport, transpiration and weight loss in a perforated modified atmosphere packaging for feijoa fruits. *Biosystems Engineering, 151*, 218–230. https://doi.org/10.1016/j.biosystemseng.2016.08.015

Castro-Yobal, M. A., Contreras-Oliva, A., Saucedo-Rivalcoba, V., Rivera-Armenta, J. L., Hernández-Ramírez, G., Salinas-Ruiz, J., et al. (2021). Evaluation of physicochemical properties of film-based alginate for food packing applications. *E-Polymers, 21*(1), 82–95. https://doi.org/10.1515/epoly-2021-0011

Chamas, A., Moon, H., Zheng, J., Qiu, Y., Tabassum, T., Jang, J. H., et al. (2020). Degradation rates of plastics in the environment. *ACS Sustainable Chemistry & Engineering, 8*(9), 3494–3511. https://doi.org/10.1021/acssuschemeng.9b06635

Chandan Kumar, D., & Vasanthi, P. (2022). Characterization of paver blocks using eggshell powder. *Materials Today: Proceedings, 68*, 1658–1662. https://doi.org/10.1016/j.matpr.2022.08.120

Chen, J., Wu, A., Yang, M., Ge, Y., Pristijono, P., Li, J., et al. (2021). Characterization of sodium alginate-based films incorporated with thymol for fresh-cut apple packaging. *Food Control, 126*, Article 108063. https://doi.org/10.1016/j.foodcont.2021.108063

Chia, W. Y., Ying Tang, D. Y., Khoo, K. S., Kay Lup, A. N., & Chew, K. W. (2020). Nature's fight against plastic pollution: Algae for plastic biodegradation and bioplastics production. *Environmental Science and Ecotechnology, 4*, Article 100065. https://doi.org/10.1016/j.ese.2020.100065

Choi, I., Shin, D., Lyu, J. S., Lee, J.-S., Song, H., Chung, M.-N., et al. (2022). Physicochemical properties and solubility of sweet potato starch-based edible films. *Food Packaging and Shelf Life, 33*, Article 100867. https://doi.org/10.1016/j.fpsl.2022.100867

Clark, R. (1995). Reflectance spectra. In T. Ahrens (Ed.), *Rock physics & phase relations: A handbook of physical constants* (pp. 178–188). USA: American Geophysical Union. Washington D.C.

Dehghani, S., Hosseini, S. V., & Regenstein, J. M. (2018). Edible films and coatings in seafood preservation: A review. *Food Chemistry, 240*, 505–513. https://doi.org/10.1016/j.foodchem.2017.07.034

Dick, M., Costa, T. M. H., Gomaa, A., Subirade, M., Rios, A. D. O., & Flôres, S. H. (2015). Edible film production from chia seed mucilage: Effect of glycerol concentration on its physicochemical and mechanical properties. *Carbohydrate Polymers, 130*, 198–205. https://doi.org/10.1016/j.carbpol.2015.05.040

Dong, Y., Chen, H., Qiao, P., & Liu, Z. (2019). Development and properties of fish gelatin/oxidized starch double network film catalyzed by thermal treatment and Schiff' base reaction. *Polymers, 11*(12), 2065. https://doi.org/10.3390/polym11122065

Douce, J., Boilot, J.-P., Biteau, J., Scodellaro, L., & Jimenez, A. (2004). Effect of filler size and surface condition of nano-sized silica particles in polysiloxane coatings. *Thin Solid Films, 466*(1–2), 114–122. https://doi.org/10.1016/j.tsf.2004.03.024

El Bourakadi, K., Mekhzoum, M. E. M., Qaiss, A. E. K., & Bouhfid, R. (2021). Active biofilms for food packaging applications. In M. Rai, & C. A. dos Santos (Eds.), *Biopolymer-based nano films: Applications in food packaging and wound healing* (pp. 65–84). Elsevier. https://doi.org/10.1016/B978-0-12-823381-8.00016-8.

Elsabee, M. Z., & Abdou, E. S. (2013). Chitosan based edible films and coatings: A review. *Materials Science and Engineering: C, 33*(4), 1819–1841. https://doi.org/10.1016/j.msec.2013.01.010

Espíndola, S. P., Norder, B., Koper, G. J., & Picken, S. J. (2023). The glass transition temperature of heterogeneous biopolymer systems. *Biomacromolecules, 24*(4), 1627–1637. https://doi.org/10.1021/acs.biomac.2c01356

Fernández, M. S., Valenzuela, F., Arias, J. I., Neira-Carrillo, A., & Arias, J. L. (2016). Is the snail shell repair process really influenced by eggshell membrane as a template of

foreign scaffold? *Journal of Structural Biology, 196*(2), 187–196. https://doi.org/10.1016/j.jsb.2016.10.001

Ferraz, E., Gamelas, J. A. F., Coroado, J., Monteiro, C., & Rocha, F. (2018). Eggshell waste to produce building lime: Calcium oxide reactivity, industrial, environmental and economic implications. *Materials and Structures, 51*, 115. https://doi.org/10.1617/s11527-018-1243-7

Flury, M., & Narayan, R. (2021). Biodegradable plastic as an integral part of the solution to plastic waste pollution of the environment. *Current Opinion in Green and Sustainable Chemistry, 30*, Article 100490. https://doi.org/10.1016/j.cogsc.2021.100490

di Franco, C. R., Cyras, V. P., Busalmen, J. P., Ruseckaite, R. A., & Vázquez, A. (2004). Degradation of polycaprolactone/starch blends and composites with sisal fibre. *Polymer Degradation and Stability, 86*(1), 95–103. https://doi.org/10.1016/j.polymdegradstab.2004.02.009

Fu, G., Qiu, S. R., Orme, C. A., Morse, D. E., & De Yoreo, J. J. (2005). Acceleration of calcite kinetics by abalone nacre proteins. *Advanced Materials, 17*(22), 2678–2683. https://doi.org/10.1002/adma.200500633

Garavito, J., Herrera, A. O., & Castellanos, D. A. (2021). A combined mathematical model to represent transpiration, respiration, and water activity changes in fresh cape gooseberry (*Physalis peruviana*) fruits. *Biosystems Engineering, 208*, 152–163. https://doi.org/10.1016/j.biosystemseng.2021.05.015

Gautron, J., Stapane, L., Le Roy, N., Nys, Y., Rodriguez-Navarro, A. B., & Hincke, M. T. (2021). Avian eggshell biomineralization: An update on its structure, mineralogy and protein tool kit. *BMC Molecular and Cell Biology, 22*, 11. https://doi.org/10.1186/s12860-021-00350-0

Gbadeyan, O. J., Adali, S., Bright, G., Sithole, B., & Awogbemi, O. (2020). Studies on the mechanical and absorption properties of *achatina fulica snail* and eggshells reinforced composite materials. *Composite Structures, 239*, Article 112043. https://doi.org/10.1016/j.compstruct.2020.112043

Ghorbani, M., & Sabour, M. R. (2021). Global trends and characteristics of vermicompost research over the past 24 years. *Environmental Science and Pollution Research, 28*, 94–102. https://doi.org/10.1007/s11356-020-11119-x

Gieroba, B., Krysa, M., Wojtowicz, K., Wiater, A., Pleszczyńska, M., Tomczyk, M., et al. (2020). The FT-IR and Raman spectroscopies as tools for biofilm characterization created by cariogenic streptococci. *International Journal of Molecular Sciences, 21*(11), 3811. https://doi.org/10.3390/ijms21113811

Gonçalves, S. M., dos Santos, D. C., Motta, J. F. G., dos Santos, R. R., Chávez, D. W. H., & de Melo, N. R. (2019). Structure and functional properties of cellulose acetate films incorporated with glycerol. *Carbohydrate Polymers, 209*, 190–197. https://doi.org/10.1016/j.carbpol.2019.01.031

Gong, Y., Han, G. T., Zhang, Y. M., Zhang, J. F., Jiang, W., Tao, X. W., et al. (2016). Preparation of alginate membrane for tissue engineering. *Journal of Polymer Engineering, 36*(4), 363–370. https://doi.org/10.1515/polyeng-2015-0065

Gontard, N., Guilbert, S., & Cuq, J.-L. (1992). Edible wheat gluten films: Influence of the main process variables on film properties using response surface methodology. *Journal of Food Science, 57*(1), 190–195. https://doi.org/10.1111/j.1365-2621.1992.tb05453.x

Grainger, D. W., & Castner, D. G. (2017). Surface analysis and biointerfaces: Vacuum and ambient in situ techniques. In P. Ducheyne (Ed.), *Comprehensive biomaterials II* (Vol. 3, pp. 1–24). Elsevier. https://doi.org/10.1016/B978-0-12-803581-8.10215-2.

Guo, L., Xu, G., Xu, C., Cheng, G., & Ding, J. (2021). Egg albumen-based biopolymer electrolyte lateral capacitive coupling thin-film transistors on logical operation. *Organic Electronics, 93*, Article 106109. https://doi.org/10.1016/j.orgel.2021.106109

Guru, P. S., & Dash, S. (2014). Sorption on eggshell waste—a review on ultrastructure, biomineralization and other applications. *Advances in Colloid and Interface Science, 209*, 49–67. https://doi.org/10.1016/j.cis.2013.12.013

Han, K., Liu, Y., Liu, Y., Huang, X., & Sheng, L. (2020). Characterization and film-forming mechanism of egg white/pullulan blend film. *Food Chemistry, 315*, Article 126201. https://doi.org/10.1016/j.foodchem.2020.126201

Hazarika, J., & Khwairakpam, M. (2022). Valorization of industrial solid waste through novel biological treatment methods – integrating different composting techniques. In C. Hussain, & S. Hait (Eds.), *Advanced organic waste management* (pp. 77–93). Elsevier. https://doi.org/10.1016/B978-0-323-85792-5.00012-5.

Her, S., Park, J., Li, P., & Bae, S. (2022). Feasibility study on utilization of pulverized eggshell waste as an alternative to limestone in raw materials for Portland cement clinker production. *Construction and Building Materials, 324*, Article 126589. https://doi.org/10.1016/j.conbuildmat.2022.126589

Ho, W.-F., Hsu, H.-C., Hsu, S.-K., Hung, C.-W., & Wu, S.-C. (2013). Calcium phosphate bioceramics synthesized from eggshell powders through a solid state reaction. *Ceramics International, 39*(6), 6467–6473. https://doi.org/10.1016/j.ceramint.2013.01.076

Ionita, M., Pandele, M. A., & Iovu, H. (2013). Sodium alginate/graphene oxide composite films with enhanced thermal and mechanical properties. *Carbohydrate Polymers, 94*(1), 339–344. https://doi.org/10.1016/j.carbpol.2013.01.065

Iyer, K. A., & Torkelson, J. M. (2014). Green composites of polypropylene and eggshell: Effective biofiller size reduction and dispersion by single-step processing with solid-state shear pulverization. *Composites Science and Technology, 102*, 152–160. https://doi.org/10.1016/j.compscitech.2014.07.029

Jalili-Firoozinezhad, S., Filippi, M., Mohabatpour, F., Letourneur, D., & Scherberich, A. (2020). Chicken egg white: Hatching of a new old biomaterial. *Materials Today, 40*, 193–214. https://doi.org/10.1016/j.mattod.2020.05.022

Jambeck, J. R., Geyer, R., Wilcox, C., Siegler, T. R., Perryman, M., Andrady, A., et al. (2015). Plastic waste inputs from land into the ocean. *Science, 347*(6223), 768–771. https://doi.org/10.1126/science.1260352

Jazie, A. A., Sinha, A. S. K., & Pramanik, H. (2013). Egg shell as eco-friendly catalyst for transesterification of rapeseed oil: Optimization for Biodiesel production. *International Journal of Biomass & Renewables, 1*, 9–18.

Jiménez, A., Fabra, M. J., Talens, P., & Chiralt, A. (2010). Effect of lipid self-association on the microstructure and physical properties of hydroxypropyl-methylcellulose edible films containing fatty acids. *Carbohydrate Polymers, 82*(3), 585–593. https://doi.org/10.1016/j.carbpol.2010.05.014

Jost, V., Kobsik, K., Schmid, M., & Noller, K. (2014). Influence of plasticiser on the barrier, mechanical and grease resistance properties of alginate cast films. *Carbohydrate Polymers, 110*, 309–319. https://doi.org/10.1016/j.carbpol.2014.03.096

Jouki, M., Khazaei, N., Ghasemlou, M., & HadiNezhad, M. (2013). Effect of glycerol concentration on edible film production from cress seed carbohydrate gum. *Carbohydrate Polymers, 96*(1), 39–46. https://doi.org/10.1016/j.carbpol.2013.03.077

Kok, J. M.-L., & Wong, C.-L. (2018). Physicochemical properties of edible alginate film from Malaysian *Sargassum polycystum* C. *Agardh. Sustainable Chemistry and Pharmacy, 9*, 87–94. https://doi.org/10.1016/j.scp.2018.07.001

Lavers, J. L., Stivaktakis, G., Hutton, I., & Bond, A. L. (2019). Detection of ultrafine plastics ingested by seabirds using tissue digestion. *Marine Pollution Bulletin, 142*, 470–474. https://doi.org/10.1016/j.marpolbul.2019.04.001

Lawrie, G., Keen, I., Drew, B., Chandler-Temple, A., Rintoul, L., Fredericks, P., et al. (2007). Interactions between alginate and chitosan biopolymers characterized using FTIR and XPS. *Biomacromolecules, 8*(8), 2533–2541. https://doi.org/10.1021/bm070014y

Liang, J., Wang, R., & Chen, R. (2019). The impact of cross-linking mode on the physical and antimicrobial properties of a chitosan/bacterial cellulose composite. *Polymers, 11*(3), 491. https://doi.org/10.3390/polym11030491

Lin, Y., Chen, H., Chan, C.-M., & Wu, J. (2008). High impact toughness polypropylene/$CaCO_3$ nanocomposites and the toughening mechanism. *Macromolecules, 41*(23), 9204–9213. https://doi.org/10.1021/ma801095d

Li, X., Ren, Z., Wang, R., Liu, L., Zhang, J., Ma, F., et al. (2021). Characterization and antibacterial activity of edible films based on carboxymethyl cellulose, *Dioscorea opposita* mucilage, glycerol and ZnO nanoparticles. *Food Chemistry, 349*, Article 129208. https://doi.org/10.1016/j.foodchem.2021.129208

Liu, Y., Cai, Z., Ma, M., Sheng, L., & Huang, X. (2020). Effect of eggshell membrane as porogen on the physicochemical structure and protease immobilization of chitosan-based macroparticles. *Carbohydrate Polymers, 242*, Article 116387. https://doi.org/10.1016/j.carbpol.2020.116387

Liu, D., Tian, H., Jia, X., & Zhang, L. (2008). Effects of calcium carbonate polymorph on the structure and properties of soy protein-based nanocomposites. *Macromolecular Bioscience, 8*(5), 401–409. https://doi.org/10.1002/mabi.200700217

Long, F., Adams, R., DeVore, D., & Franklin, M. (2004). *Therapeutic, nutraceutical and cosmetic applications for eggshell membrane and processed eggshell membrane preparations.* U.S. Patent US2004/0180025A1.

López, O. V., Ninago, M. D., Lencina, M. M. S., García, M. A., Andreucetti, N. A., Ciolino, A. E., et al. (2015). Thermoplastic starch plasticized with alginate–glycerol mixtures: Melt-processing evaluation and film properties. *Carbohydrate Polymers, 126*, 83–90. https://doi.org/10.1016/j.carbpol.2015.03.030

Lucas, J. C., Borrajo, J., & Williams, R. J. (1993). Cure of unsaturated polyester resins: 2. Influence of low-profile additives and fillers on the polymerization reaction, mechanical properties and surface rugosities. *Polymer, 34*(9), 1886–1890. https://doi.org/10.1016/0032-3861(93)90430-I

Lunn, J., & Buttriss, J. L. (2007). Carbohydrates and dietary fibre. *Nutrition Bulletin, 32*(1), 21–64. https://doi.org/10.1111/j.1467-3010.2007.00616.x

Luo, Y., Liu, H., Yang, S., Zeng, J., & Wu, Z. (2019). Sodium alginate-based green packaging films functionalized by guava leaf extracts and their bioactivities. *Materials, 12*(18), 2923. https://doi.org/10.3390/ma12182923

Mahcene, Z., Khelil, A., Hasni, S., Akman, P. K., Bozkurt, F., Birech, K., et al. (2020). Development and characterization of sodium alginate based active edible films incorporated with essential oils of some medicinal plants. *International Journal of Biological Macromolecules, 145*, 124–132. https://doi.org/10.1016/j.ijbiomac.2019.12.093

Marangoni Júnior, L., Rodrigues, P. R., da Silva, R. G., Vieira, R. P., & Alves, R. M. V. (2021). Sustainable packaging films composed of sodium alginate and hydrolyzed collagen: Preparation and characterization. *Food and Bioprocess Technology, 14*, 2336–2346. https://doi.org/10.1007/s11947-021-02727-7

Masuda, Y., & Hiramatsu, H. (2007). Bioavailability and physiological function of eggshells and eggshell membranes. In Y. Mine (Ed.), *Egg bioscience and biotechnology* (pp. 129–140). John Wiley & Sons, Inc. https://doi.org/10.1002/9780470181249.ch3.

Mei, J., Yuan, Y., Wu, Y., & Li, Y. (2013). Characterization of edible starch–chitosan film and its application in the storage of Mongolian cheese. *International Journal of Biological Macromolecules, 57*, 17–21. https://doi.org/10.1016/j.ijbiomac.2013.03.003

Mohammadi, R., Mohammadifar, M. A., Rouhi, M., Kariminejad, M., Mortazavian, A. M., Sadeghi, E., et al. (2018). Physico-mechanical and structural properties of eggshell membrane gelatin- chitosan blend edible films. *International Journal of Biological Macromolecules, 107*, 406–412. https://doi.org/10.1016/j.ijbiomac.2017.09.003

Moharir, R. V., & Kumar, S. (2019). Challenges associated with plastic waste disposal and allied microbial routes for its effective degradation: A comprehensive review. *Journal of Cleaner Production, 208*, 65–76. https://doi.org/10.1016/j.jclepro.2018.10.059

Molavi, H., Behfar, S., Ali Shariati, M., Kaviani, M., & Atarod, S. (2015). A review on biodegradable starch based film. *Journal of Microbiology, Biotechnology and Food Sciences, 4*(5), 456–461. https://doi.org/10.15414/jmbfs.2015.4.5.456-461

Naemchan, K., Meejoo, S., Onreabroy, W., & Limsuwan, P. (2008). Temperature effect on chicken egg shell investigated by XRD, TGA and FTIR. *Advanced Materials Research, 55–57*, 333–336. https://doi.org/10.4028/www.scientific.net/AMR.55-57.333.

Naidu, D. S., & John, M. J. (2021). Cellulose nanofibrils reinforced xylan-alginate composites: Mechanical, thermal and barrier properties. *International Journal of Biological Macromolecules, 179*, 448–456. https://doi.org/10.1016/j.ijbiomac.2021.03.035

Nakano, T., Ikawa, N., & Ozimek, L. (2003). Chemical composition of chicken eggshell and shell membranes. *Poultry Science, 82*(3), 510–514. https://doi.org/10.1093/ps/82.3.510

Nordin, N., Othman, S. H., Rashid, S. A., & Basha, R. K. (2020). Effects of glycerol and thymol on physical, mechanical, and thermal properties of corn starch films. *Food Hydrocolloids, 106*, Article 105884. https://doi.org/10.1016/j.foodhyd.2020.105884

Nys, Y., Gautron, J., Garcia-Ruiz, J. M., & Hincke, M. T. (2004). Avian eggshell mineralization: Biochemical and functional characterization of matrix proteins. *Comptes Rendus Palevol, 3*(6–7), 549–562. https://doi.org/10.1016/j.crpv.2004.08.002

Oluic, A. J., & Holmquist, J. (2021). Overcoming the challenges of producing a quality water-soluble film. *Reinforced Plastics, 65*(4), 198–202. https://doi.org/10.1016/j.repl.2020.12.001

Osman, M. A., Atallah, A., & Suter, U. W. (2004). Influence of excessive filler coating on the tensile properties of LDPE–calcium carbonate composites. *Polymer, 45*(4), 1177–1183. https://doi.org/10.1016/j.polymer.2003.12.020

Paşcalău, V., Popescu, V., Popescu, G. L., Dudescu, M. C., Borodi, G., Dinescu, A., et al. (2012). The alginate/k-carrageenan ratio's influence on the properties of the cross-linked composite films. *Journal of Alloys and Compounds, 536*, S418–S423. https://doi.org/10.1016/j.jallcom.2011.12.026

Pasquali, I., Andanson, J.-M., Kazarian, S. G., & Bettini, R. (2008). Measurement of CO_2 sorption and PEG 1500 swelling by ATR-IR spectroscopy. *The Journal of Supercritical Fluids, 45*(3), 384–390. https://doi.org/10.1016/j.supflu.2008.01.015

Pavlath, A. E., & Orts, W. (2009). Edible films and coatings: Why, what, and how? In K. C. Huber, & M. E. Embuscado (Eds.), *Edible films and coatings for food applications* (pp. 1–23). Springer New York. https://doi.org/10.1007/978-0-387-92824-1_1.

Pelissari, F. M., Andrade-Mahecha, M. M., Sobral, P. J. do A., & Menegalli, F. C. (2013). Comparative study on the properties of flour and starch films of plantain bananas (*Musa paradisiaca*). *Food Hydrocolloids, 30*(2), 681–690. https://doi.org/10.1016/j.foodhyd.2012.08.007

Prapruddivongs, C., & Wongpreedee, T. (2020). Use of eggshell powder as a potential hydrolytic retardant for citric acid-filled thermoplastic starch. *Powder Technology, 370*, 259–267. https://doi.org/10.1016/j.powtec.2020.05.076

Rahman, M. M., Netravali, A. N., Tiimob, B. J., & Rangari, V. K. (2014). Bioderived "green" composite from soy protein and eggshell nanopowder. *ACS Sustainable Chemistry & Engineering, 2*(10), 2329–2337. https://doi.org/10.1021/sc5003193

Raza, S. T., Wu, J., Rene, E. R., Ali, Z., & Chen, Z. (2022). Application of wetland plant-based vermicomposts as an organic amendment with high nutritious value. *Process Safety and Environmental Protection, 165*, 941–949. https://doi.org/10.1016/j.psep.2022.04.025

Roy, S., & Rhim, J.-W. (2020). Effect of CuS reinforcement on the mechanical, water vapor barrier, UV-light barrier, and antibacterial properties of alginate-based composite films. *International Journal of Biological Macromolecules, 164*, 37–44. https://doi.org/10.1016/j.ijbiomac.2020.07.092

Salimi, A., Alavehzadeh, A., Ramezani, M., & Pourahmad, J. (2022). Differences in sensitivity of human lymphocytes and fish lymphocytes to polyvinyl chloride microplastic toxicity. *Toxicology and Industrial Health, 38*(2), 100–111. https://doi.org/10.1177/074823372110658

Samal, K., Raj Mohan, A., Chaudhary, N., & Moulick, S. (2019). Application of vermitechnology in waste management: A review on mechanism and performance. *Journal of Environmental Chemical Engineering, 7*(5), Article 103392. https://doi.org/10.1016/j.jece.2019.103392

Sampath Kumar, T. S., Madhumathi, K., Rajkamal, B., Zaheatha, S., Rajathi Malar, A., & Alamelu Bai, S. (2014). Enhanced protein delivery by multi-ion containing eggshell derived apatitic-alginate composite nanocarriers. *Colloids and Surfaces B: Biointerfaces, 123*, 542–548. https://doi.org/10.1016/j.colsurfb.2014.09.052

Santos, K. O., Barbosa, R. C., da Silva Buriti, J., Bezerra Junior, A. G., de Sousa, W. J. B., de Barros, S. M. C., et al. (2019). Thermal, chemical, biological and mechanical properties of chitosan films with powder of eggshell membrane for biomedical applications. *Journal of Thermal Analysis and Calorimetry, 136*, 725–735. https://doi.org/10.1007/s10973-018-7666-0

Saravanakumar, K., Sathiyaseelan, A., Mariadoss, A. V. A., Xiaowen, H., & Wang, M. H. (2020). Physical and bioactivities of biopolymeric films incorporated with cellulose, sodium alginate and copper oxide nanoparticles for food packaging application. *International Journal of Biological Macromolecules, 153*, 207–214. https://doi.org/10.1016/j.ijbiomac.2020.02.250

Sathiparan, N. (2021). Utilization prospects of eggshell powder in sustainable construction material – a review. *Construction and Building Materials, 293*, Article 123465. https://doi.org/10.1016/j.conbuildmat.2021.123465

Schaafsma, A., Pakan, I., Hofstede, G. J. H., Muskiet, F. A., Van Der Veer, E., & De Vries, P. J. F. (2000). Mineral, amino acid, and hormonal composition of chicken eggshell powder and the evaluation of its use in human nutrition. *Poultry Science, 79*(12), 1833–1838. https://doi.org/10.1093/ps/79.12.1833

Seeharaj, P., Sripako, K., Promta, P., Detsri, E., & Vittayakorn, N. (2019). Facile and eco-friendly fabrication of hierarchical superhydrophobic coating from eggshell biowaste. *International Journal of Applied Ceramic Technology, 16*(5), 1895–1903. https://doi.org/10.1111/ijac.13235

Seifan, M., Samani, A. K., Hewitt, S., & Berenjian, A. (2017). The effect of cell immobilization by calcium alginate on bacterially induced calcium carbonate precipitation. *Fermentation, 3*(4), 57. https://doi.org/10.3390/fermentation3040057

Shankar, S., Wang, L.-F., & Rhim, J.-W. (2017). Preparation and properties of carbohydrate-based composite films incorporated with CuO nanoparticles. *Carbohydrate Polymers, 169*, 264–271. https://doi.org/10.1016/j.carbpol.2017.04.025

Sharma, K., & Garg, V. K. (2017). Management of food and vegetable processing waste spiked with buffalo waste using earthworms (*Eisenia fetida*). *Environmental Science and Pollution Research, 24*, 7829–7836. https://doi.org/10.1007/s11356-017-8438-2

Sharma, K., & Garg, V. K. (2019). Vermicomposting of waste: A zero-waste approach for waste management. In M. J. Taherzadeh, K. Bolton, J. Wong, & A. Pandey (Eds.), *Sustainable resource recovery and zero waste approaches* (pp. 133–164). Elsevier. https://doi.org/10.1016/B978-0-444-64200-4.00010-4.

Shiferaw, N., Habte, L., Thenepalli, T., & Ahn, J. W. (2019). Effect of eggshell powder on the hydration of cement paste. *Materials, 12*(15), 2483. https://doi.org/10.3390/ma12152483

Soares, J. P., Santos, J. E., Chierice, G. O., & Cavalheiro, E. T. G. (2004). Thermal behavior of alginic acid and its sodium salt. *Ecletica Quimica, 29*(2), 57–63. https://doi.org/10.1590/s0100-46702004000200009

de Spelta, J. S. O., & de Galdino, A. G. S. (2018). Bioceramic composite: hen's eggshell characterization and main applications. *Revista Ifes Ciência, 4*(1), 9–20. https://doi.org/10.36524/ric.v4i1.323

Stoica, M., Marian Antohi, V., Laura Zlati, M., & Stoica, D. (2020). The financial impact of replacing plastic packaging by biodegradable biopolymers - a smart solution for the food industry. *Journal of Cleaner Production, 277*, Article 124013. https://doi.org/10.1016/j.jclepro.2020.124013

Swati, A., & Hait, S. (2018). Greenhouse gas emission during composting and vermicomposting of organic wastes - a review. *Clean - Soil, Air, Water, 46*(6), Article 1700042. https://doi.org/10.1002/clen.201700042

Tang, S., Zou, P., Xiong, H., & Tang, H. (2008). Effect of nano-SiO_2 on the performance of starch/polyvinyl alcohol blend films. *Carbohydrate Polymers, 72*(3), 521–526. https://doi.org/10.1016/j.carbpol.2007.09.019

Taylor, D., Walsh, M., Cullen, A., & O'Reilly, P. (2016). The fracture toughness of eggshell. *Acta Biomaterialia, 37*, 21–27. https://doi.org/10.1016/j.actbio.2016.04.028

Teixeira, S. C., Silva, R. R. A., de Oliveira, T. V., Stringheta, P. C., Pinto, M. R. M. R., & Soares, N. de F. F. (2021). Glycerol and triethyl citrate plasticizer effects on molecular, thermal, mechanical, and barrier properties of cellulose acetate films. *Food Bioscience, 42*, Article 101202. https://doi.org/10.1016/j.fbio.2021.101202

Tongdeesoontorn, W., Mauer, L. J., Wongruong, S., Sriburi, P., & Rachtanapun, P. (2011). Effect of carboxymethyl cellulose concentration on physical properties of biodegradable cassava starch-based films. *Chemistry Central Journal, 5*, 6. https://doi.org/10.1186/1752-153X-5-6

UNEP United Nations Environment Programme. (2022). *Beat plastic pollution*. Retrieved from https://www.unep.org/interactives/beat-plastic-pollution/. (Accessed 6 October 2022) Accessed.

Valenzuela, C., Abugoch, L., & Tapia, C. (2013). Quinoa protein-chitosan-sunflower oil edible film: Mechanical, barrier and structural properties. *LWT - Food Science and Technology, 50*(2), 531–537. https://doi.org/10.1016/j.lwt.2012.08.010

Valenzuela, C., Abugoch, L., Tapia, C., & Gamboa, A. (2013). Effect of alkaline extraction on the structure of the protein of quinoa (*Chenopodium quinoa* Willd.) and its influence on film formation. *International Journal of Food Science and Technology, 48*(4), 843–849. https://doi.org/10.1111/ijfs.12035

Valenzuela, C., Tapia, C., López, L., Bunger, A., Escalona, V., & Abugoch, L. (2015). Effect of edible quinoa protein-chitosan based films on refrigerated strawberry (*Fragaria* × *ananassa*) quality. *Electronic Journal of Biotechnology, 18*(6), 406–411. https://doi.org/10.1016/j.ejbt.2015.09.001

Valero, A. (2013). *Principios de color y holopintura*. Alicante, España: Editorial Club Universitario (Chapter 5).

Vattanagijyingyong, Y., Yonemochi, E., & Chatchawalsaisin, J. (2021). Miscibility characterization of zein/methacrylic acid copolymer composite films and plasticization effects. *International Journal of Pharmaceutics, 601*, Article 120498. https://doi.org/10.1016/j.ijpharm.2021.120498

Verma, R., Vinoda, K. S., Papireddy, M., & Gowda, A. N. S. (2016). Toxic pollutants from plastic waste- A review. *Procedia Environmental Sciences, 35*, 701–708. https://doi.org/10.1016/j.proenv.2016.07.069

Vig, A. P., Singh, J., Wani, S. H., & Singh Dhaliwal, S. (2011). Vermicomposting of tannery sludge mixed with cattle dung into valuable manure using earthworm *Eisenia fetida* (Savigny). *Bioresource Technology, 102*(17), 7941–7945. https://doi.org/10.1016/j.biortech.2011.05.056

Vinod, A., Sanjay, M. R., Suchart, S., & Jyotishkumar, P. (2020). Renewable and sustainable biobased materials: An assessment on biofibers, biofilms, biopolymers and biocomposites. *Journal of Cleaner Production, 258*, Article 120978. https://doi.org/10.1016/j.jclepro.2020.120978

Vonnie, J. M., Rovina, K., Azhar, R. A., Huda, N., Erna, K. H., Felicia, W. X. L., et al. (2022). Development and characterization of the biodegradable film derived from eggshell and cornstarch. *Journal of Functional Biomaterials, 13*(2), 67. https://doi.org/10.3390/jfb13020067

Waheed, M., Yousaf, M., Shehzad, A., Inam-Ur-Raheem, M., Khan, M. K. I., Khan, M. R., et al. (2020). Channelling eggshell waste to valuable and utilizable products: A comprehensive review. *Trends in Food Science & Technology, 106*, 78–90. https://doi.org/10.1016/j.tifs.2020.10.009

Wang, H., Ding, F., Ma, L., & Zhang, Y. (2021). Edible films from chitosan-gelatin: Physical properties and food packaging application. *Food Bioscience, 40*, Article 100871. https://doi.org/10.1016/j.fbio.2020.100871

Wen, G., Huang, J., & Guo, Z. (2019). Energy-effective superhydrophobic nanocoating based on recycled eggshell. *Colloids and Surfaces A: Physicochemical and Engineering Aspects, 568*, 20–28. https://doi.org/10.1016/j.colsurfa.2019.01.067

Wright, S. L., & Kelly, F. J. (2017). Plastic and human health: A micro issue? *Environmental Science & Technology, 51*(12), 6634–6647. https://doi.org/10.1021/acs.est.7b00423

Xiao, Q., Gu, X., & Tan, S. (2014). Drying process of sodium alginate films studied by two-dimensional correlation ATR-FTIR spectroscopy. *Food Chemistry, 164*, 179–184. https://doi.org/10.1016/j.foodchem.2014.05.044

Yang, M., Shi, J., & Xia, Y. (2018). Effect of SiO_2, PVA and glycerol concentrations on chemical and mechanical properties of alginate-based films. *International Journal of Biological Macromolecules, 107*, 2686–2694. https://doi.org/10.1016/j.ijbiomac.2017.10.162

Yew, M. C., Ramli Sulong, N. H., Yew, M. K., Amalina, M. A., & Johan, M. R. (2013). The formulation and study of the thermal stability and mechanical properties of an acrylic coating using chicken eggshell as a novel bio-filler. *Progress in Organic Coatings, 76*(11), 1549–1555. https://doi.org/10.1016/j.porgcoat.2013.06.011

Yoo, S., Hsieh, J. S., Zou, P., & Kokoszka, J. (2009). Utilization of calcium carbonate particles from eggshell waste as coating pigments for ink-jet printing paper. *Bioresource Technology, 100*(24), 6416–6421. https://doi.org/10.1016/j.biortech.2009.06.112

Yuan, Z., Nag, R., & Cummins, E. (2022). Human health concerns regarding microplastics in the aquatic environment - from marine to food systems. *Science of the Total Environment, 823*, Article 153730. https://doi.org/10.1016/j.scitotenv.2022.153730

Zhang, H., Peng, M., Cheng, T., Zhao, P., Qiu, L., Zhou, J., et al. (2018). Silver nanoparticles-doped collagen–alginate antimicrobial biocomposite as potential wound dressing. *Journal of Materials Science, 53*, 14944–14952. https://doi.org/10.1007/s10853-018-2710-9

Zhao, Y., Huang, Z., Zhang, J., Wu, W., Wang, M., & Fan, L. (2010). Thermal degradation of sodium alginate- incorporated soy protein isolate/glycerol composite membranes. In *Proceedings of the 17th IAPRI world conference on packaging* (pp. 402–405).

Zhou, Y., Li, H., Guo, W., Liu, H., & Cai, M. (2022). The synergistic effect between biofertility properties and biological activities in vermicomposting: A comparable study of pig manure. *Journal of Environmental Management, 324*, Article 116280. https://doi.org/10.1016/j.jenvman.2022.116280